https://doi.org/10.5194/egusphere-2025-6010
Preprint. Discussion started: 17 December 2025
© Author(s) 2025. CC BY 4.0 License.

Climate Controls on Snowfall at Coastal West Antarctic Ice Rises - Potential Ice Core Sites

Julia R. Andreasen[1,2], Peter D. Neff[1]

[1]Department of Soil, Water, and Climate, University of Minnesota Twin Cities, Saint Paul, MN, USA
[2]International Arctic Research Center, University of Alaska Fairbanks, Fairbanks, AK, USA

Correspondence to: Julia R. Andreasen (jrandreasen@alaska.edu)

Abstract. The West Antarctic Ice Sheet (WAIS) is a dynamic system where interactions between ice, ocean, and atmosphere drive significant ice mass loss, raising concerns of irreversible retreat and sea-level rise. Long-term observational records of variability and change along the WAIS coast are largely restricted to satellite observations, but more direct observations are needed, given this region's present and future societal impact. Coastal ice rises, grounded domes of ice embedded in or along the margins of ice shelves, preserve in their accumulated snowfall high-resolution records of past climate variability that can be recovered by ice coring. These potential ice core sites offer unique opportunities to reconstruct key drivers of regional change, including modes of atmosphere-ocean variability described by the Southern Annular Mode (SAM), the Amundsen Sea Low (ASL), and El Niño–Southern Oscillation (ENSO)—and warrant exploration via climate reanalysis to assess the relative balance of climate controls at any potential ice core site. This study uses ERA5 and MERRA-2 reanalysis to evaluate the climate controls on interannual snowfall variability at thirteen WAIS coastal ice rises over the satellite era (1979–2022). Results highlight longitudinal differences in how interannual snowfall variability at coastal ice rises is influenced by SAM, ENSO, and Bellingshausen Sea atmospheric pressure anomalies. Snow accumulation (precipitation) as resolved in atmospheric reanalysis suggests that, as potential ice core sites, Dean Island and Guest Peninsula, located in the West Sector of the WAIS coast, are strongly influenced by broad Southern Hemisphere westerly wind anomalies suppressing local precipitation, making them ideal for isolating this mode of variability in paleoclimate reconstructions. In contrast, Farwell Island in the East Sector exhibits a positive relationship between precipitation and cyclonic activity associated with Bellingshausen Sea pressure variability, making it a key site for reconstructing the influence of synoptic-scale pressure systems on coastal accumulation in this region. These findings inform future ice core studies aimed at understanding WAIS climate dynamics, with implications for projections of Antarctic stability and global sea-level rise.

1 Introduction

1.1 Significance of the WAIS Coast and its Data Gap

The West Antarctic Ice Sheet (WAIS) is a pivotal region in the global climate system due to its vulnerability to ice loss, possible tipping-point behavior, and its potential to drive substantial sea-level rise in coming decades and centuries (Bamber

https://doi.org/10.5194/egusphere-2025-6010
Preprint. Discussion started: 17 December 2025
© Author(s) 2025. CC BY 4.0 License.

et al., 2009; Mercer, 1978). Rapid ice discharge from particularly concerning Amundsen Sea regional outlet glaciers, including Thwaites and Pine Island Glaciers, is in response to a complex confluence of interactions between atmospheric, oceanic, and ice-sheet processes (Joughin & Alley, 2011). These dynamics are amplified by the WAIS's bed geometry: much of its ice rests below sea level, making it prone to instability and irreversible retreat. Understanding both present and past ice-ocean-atmosphere interactions is critical to predicting future changes in this region (Barr & Lovell, 2014; Joughin et al., 2014; Steig & Neff, 2018).

Observations since the mid-20th century reveal regional warming air temperatures (Li et al., 2021; Steig et al., 2009) and variable snow accumulation trends across WAIS, in addition to considerable (but poorly observed) spatial and inter-annual variability (Medley & Thomas, 2019; Thomas et al., 2017). Ice cores have long been the cornerstone of Antarctic paleoclimate reconstruction, preserving high-resolution records of accumulation, temperature, atmospheric composition, and synoptic variability through a wide range of geochemical proxy approaches (Banta et al., 2008; Orsi et al., 2012; Steig et al., 2013). These stratigraphic climate archives are primarily recovered from the cold, stable interior of the East and West Antarctic Ice Sheets and have been instrumental in reconstructing late 20th-century climate conditions. Sites such as WAIS Divide, Siple Dome, and South Pole have yielded important insights into regional climate variability and accumulation changes in West Antarctica (Mayewski et al., 2004; Orsi et al., 2012; Steig et al., 2013; Winski et al., 2019). Additionally, the US ITASE project (1999–2003) established a decadal to multi-century ice core network across the Pine Island–Thwaites drainage system, the Ross drainage basin, and the central West Antarctic ice divide and revealed the sensitivity of snow accumulation to regional climate drivers, including cyclone frequency and intensity, wind direction, and topographic influence (Kaspari et al., 2004). However, the closest WAIS ITASE site is 295 km inland at 1353 m elevation (Kaspari et al., 2004), and WAIS firn cores range from 180 km inland (DIV2010) to 500 km inland (UPT2009) and above 1300 m elevation (Criscitiello et al., 2014). While conditions at these distances favor long-term stratigraphic preservation and old ice ages at depth, they are limited in their ability to capture the distinct coastal climate processes and strong spatial gradients relevant to more specific regions like the Amundsen Sea coast. This leaves a critical observational gap along the WAIS coast, one of the most climatically dynamic and glaciologically vulnerable regions of Antarctica. Here, processes such as atmospheric river landfalls, the Amundsen Sea Low, and ocean-atmosphere coupling strongly modulate accumulation and ice dynamics (Smith et al., 2020; Turner et al., 2017; Wille et al., 2019). Yet, this region remains poorly sampled by ice cores, and instrumental records only extend back to the International Geophysical Year (1957–58) in locations particularly distant from coastal West Antarctica (Byrd Station, approximately 500 km inland e.g. Bromwich et al., 2013). To better characterize the spatial and temporal variability of snow accumulation and other environmental variables in response to synoptic climate drivers such as cyclonic activity and atmospheric rivers, we are in critical need of longer and more spatially distributed records along the WAIS coast (Neff, 2020; Wille et al., 2019).

https://doi.org/10.5194/egusphere-2025-6010
Preprint. Discussion started: 17 December 2025
© Author(s) 2025. CC BY 4.0 License.

1.2 Climatological Drivers and Oceanic Interactions Along the WAIS Coast

The WAIS coast faces the Ross, Amundsen, and Bellingshausen Seas in the broader Pacific sector of the Southern Ocean, where diverse interactions between the atmosphere, ocean, and ice sheet shape snow accumulation and ice loss. North of the WAIS coast, a primary driver of regional climate is the Southern Annular Mode (SAM) a description of the position and intensity of Southern Hemisphere westerly winds, which interact with the Amundsen Sea Low (ASL), a quasi-stationary low-pressure region (Lee et al., 2019; Marshall, 2003; Thompson & Wallace, 2001) between the Ross and Amundsen Seas. SAM's negative phase weakens both westerly winds and the Amundsen Sea Low, whereas its positive (current) phase enhances cyclonic activity and modulates snowfall patterns (Figures A1 and A2), including possible increased precipitation over Ellsworth Land and reduced accumulation near the Ross Ice Shelf over the 20th century (Medley & Thomas, 2019; Winstrup et al., 2019).

El Niño–Southern Oscillation (ENSO) conditions further modulate ASL activity, with El Niño phase of ENSO occurring when warmer tropical Pacific waters send atmospheric teleconnections that deepen the ASL (Cook et al., 2016; Ding et al., 2011), modify wind stress and sea level pressure patterns, and drive northwest-to-southeast winds that transport warm, moist air to the WAIS coast and increase snow accumulation (Figure A3) (Karoly, 1989; Paolo et al., 2018). These circulation changes also facilitate Circumpolar Deep Water (CDW) transport onto the Antarctic continental shelf, facilitating its movement via bathymetric troughs along the Bellingshausen and Amundsen Sea margins into regions like Pine Island Bay, raising subsurface ocean temperatures to approximately +1°C (Petty et al., 2013). These upwelled waters drive basal ice shelf melt, ice shelf thinning, and play a role in WAIS outlet glacier grounding-line retreat (Pritchard et al., 2012; Dutrieux et al., 2014; Steig et al., 2012).

In contrast, cool tropical Pacific temperatures during La Niña phase deepen the ASL. This drives southeast-to-northwest winds and brings cold, dry air from the interior, which reduces snowfall, limits basal melt and CDW upwelling, and promotes sea ice growth (Figure A4). The interplay between ENSO and SAM introduces additional complexity, as particular combinations of the phases of these indices can amplify or mitigate snow accumulation and oceanic heat fluxes in coastal WAIS (Fogt et al., 2011). Understanding these coupled processes, including before the satellite era (~1979) via ice core paleoclimate reconstruction, is critical for improving reconstructions of WAIS coastal regions (Dalaiden et al., 2021) and projections of WAIS response to ice–ocean–atmosphere interactions and global sea-level rise.

1.3 The Role of Ice Rises

Although inland ice cores and reanalysis datasets cannot fully capture the dynamic coastal climate, particularly localized processes like synoptic-scale atmospheric forcing (O'Connor et al., 2025), ice rises offer a unique opportunity to address the paucity of climate records in coastal WAIS. These stable features are grounded on bedrock, embedded within or at the margin of ice shelves, and characterized by local snow accumulation and slow horizontal ice flow in their summit regions—ideal characteristics essentially identical to those of inland ice sheet divide locations (Dansgaard and Johnsen, 1969). Ice rises

https://doi.org/10.5194/egusphere-2025-6010
Preprint. Discussion started: 17 December 2025
© Author(s) 2025. CC BY 4.0 License.

preserve high-resolution climate records via chemical impurities in annual snow layers that can be used to reconstruct past interactions between atmospheric, oceanic, and ice-sheet processes (Matsuoka et al., 2015; Rowell et al., 2023). Many ice cores have already been recovered from Antarctic ice rises, as seen in Figure 1.

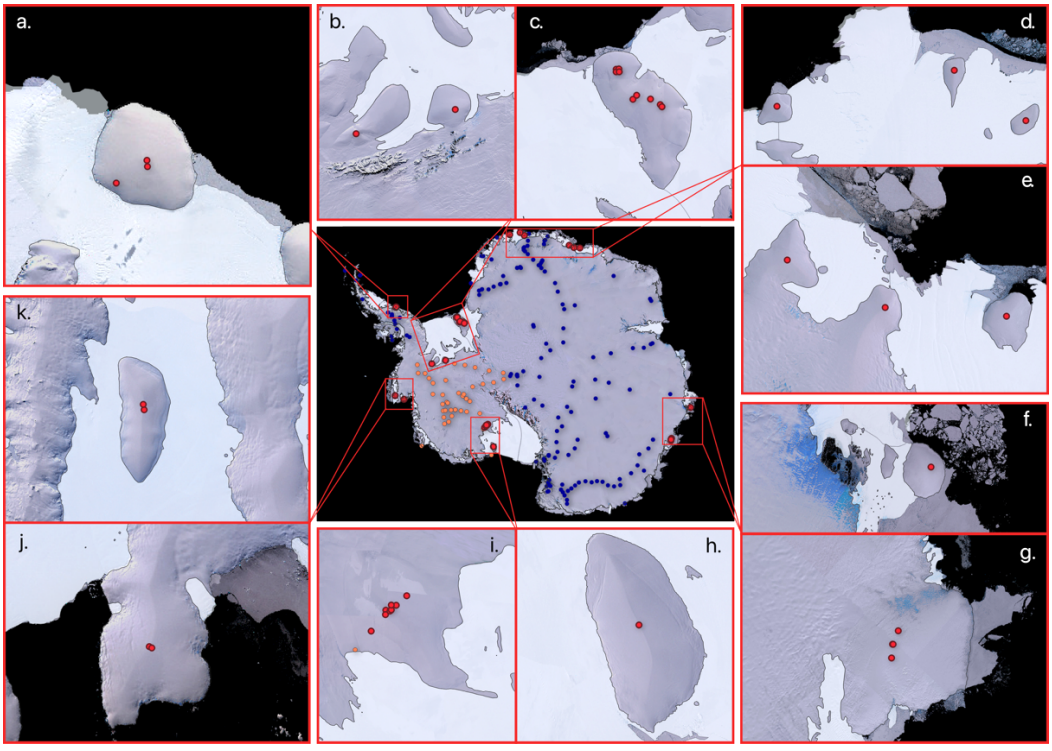

Figure 1: Antarctic ice core map featuring ice rises: red dots indicate ice rise ice core sites, orange dots indicate remaining WAIS ice core sites, and blue dots indicate remaining AP and EAIS ice core sites; a. Dolleman Island, b. Fletcher Promontory (left) and Skytrain Ice Rise (right), c. Berkner Island, d. Blåskimen Island (left), Kupol Moskovskij (center), and Kupol Ciolkovskogo (right), e. Hammarryggen ice rise (left), Lokeryggen ice rise (center), and Derwael ice rise (right), f. Mill Island, g. Law Dome, h. Roosevelt Island, i. Siple Dome, j. Canisteo Peninsula, and k. Sherman Island. The background map is the Landsat Image of Antarctica (LIMA) mosaic (Bindschadler et al., 2008).

The significance of ice rises lies in their ability to bridge the spatial and temporal gaps in existing datasets, particularly in coastal WAIS, where few climate observations or annually resolved ice core records have been recovered or developed—in fact, human observations and sustained presence are uniquely unbiased with respect to the coast in this one sector of Antarctica. Ice rises naturally preserve the integrated effects of atmospheric and oceanic variability in the thickness of and chemical impurities contained within annual snow layers (hereafter snow accumulation). Of the continent's 124 ice rises (with individual areas of at least 90 km^2), 30 of them line the WAIS coast (Matsuoka et al., 2015). These WAIS ice rises span approximately 2,600 kilometers of coastline and 75 degrees of longitude (156ºW to 82ºW) from Ellsworth Land and the southern extent of the Antarctic Peninsula to the eastern Ross Sea and King Edward VII Land (Figure 2). We split the larger ice rises (20 km by 40 km at smallest; Dean Island) into an East Sector, which includes Farwell Island (FI), Noville Peninsula (NP), Sherman

https://doi.org/10.5194/egusphere-2025-6010
Preprint. Discussion started: 17 December 2025
© Author(s) 2025. CC BY 4.0 License.

Island (SI), King Peninsula (KP), Canisteo Peninsula (CP), and Bear Peninsula (BP), and a West Sector, which includes Martin Peninsula (MP), Wright Island (WI), Carney Island (CI), Siple Island (SI), Dean Island (DI), Guest Peninsula (GP), and Roosevelt Island (RI) (Figure 2). Utilizing ice rises as ice core sites to reconstruct past climate variability along the coast would provide an ideal range of direct and proxy observations for understanding recent WAIS climate history that short, sparse observations and climate model datasets cannot currently address (Steig and Neff, 2018; Neff, 2020).

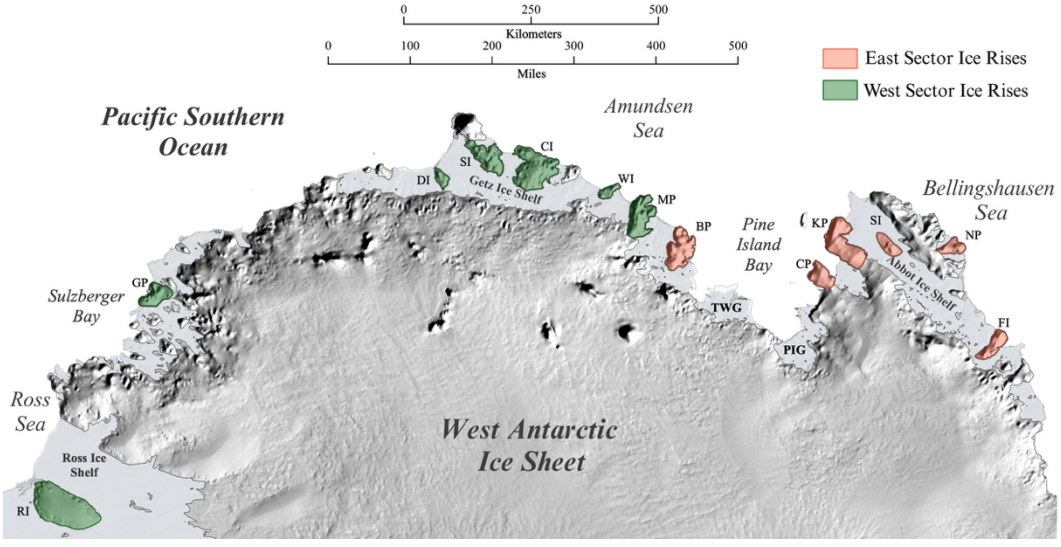

Figure 2: East and west sector ice rises along the WAIS coast, facing the Ross, Amundsen, and Bellingshausen seas, with East Sector ice rises highlighted in orange and West Sector ice rises highlighted in green; the background map is Bedmap-2 surface topography.

2 Methods

2.1 Reanalysis Datasets and Site Selection

To investigate drivers of snowfall variability across coastal West Antarctica, we utilize European Centre for Medium Range Weather Forecasts (ECMWF) Re-analysis (ERA5, resolution 35 km) data for most climate assessments and include a comparison to NASA's Modern-Era Retrospective analysis for Research and Applications, Version 2 (MERRA-2, resolution 0.625°×0.5° or ~50 km) data, focusing on precipitation, surface air temperature, wind, geopotential height, sea surface temperature (SST), sea ice concentration (SIC), and large-scale climate indices. The thirteen coastal ice rises across the Amundsen Sea sector serve as our fixed observation sites, each defined by precise latitude and longitude. We calculate the maximum height of each ice rise using MEaSUREs BedMachine Version 3 (Morlighem, 2022; Morlighem et al., 2020), with a spatial resolution of 500 m, to reflect the topographical range across the coast. Annual precipitation and temperature time series from 1979 to 2022 are extracted for each site by rounding coordinates to the nearest reanalysis grid cell (ERA5: ~0.25°, MERRA-2: ~0.5°). Additionally, the domain for broader atmospheric and oceanic averaging, the "Amundsen Sea box," is consistently defined as 72°–55°S latitude and 150°–105°W longitude, unless otherwise specified. This domain captures the

https://doi.org/10.5194/egusphere-2025-6010
Preprint. Discussion started: 17 December 2025
© Author(s) 2025. CC BY 4.0 License.

influence of the ASL and its surrounding westerly flow, based on the climatological position and variability of low-pressure centers that frequently pass through the Amundsen Sea sector (Assmann et al., 2005; Hosking et al., 2013; Turner et al., 2013). It lies within the broader region (50°W–180°W, 60°–75°S) commonly used to track the ASL in prior studies (Turner et al., 2013).

2.2 ERA5 and MERRA-2 Temperature and Precipitation Comparison

To evaluate consistency between reanalysis datasets, we compare annual 2-meter air temperature and total precipitation from ERA5 and MERRA-2 at all 13 ice rise locations. We exclude 1979 in this comparison due to MERRA-2 constraints and omit earlier years to avoid the lack of observational constraints due to sparse pre-satellite observations in the Antarctic (Bromwich et al., 2007). Pearson correlation coefficients (r) and p-values are computed for both variables at each site. To visualize spatial agreement, we expand the comparison to a gridded analysis over 60°S–90°S and 170°W–90°W. For each MERRA-2 grid cell, we locate the nearest ERA5 grid cell using great-circle distance, extract annual temperature and precipitation time series, and compute correlation statistics. Seasonal climatologies for austral summer (December-February, DJF) and winter (June-August, JJA) are also compared.

2.3 Regional Correlations

We assess how regional wind patterns influence local snowfall by correlating ERA5 precipitation with zonal (U-wind) and meridional (V-wind) wind fields averaged over two domains, the broad Amundsen box (72°–55°S, 150°–105°W) and the so-called "Steig box" (72°–68°S, 125°–100°W, Steig et al., 2012). The Steig box is a localized domain optimized to capture the specific pressure and wind anomalies most relevant to upwelling of water bodies such as Circumpolar Deep Water (CDW) onto the Antarctic continental shelf and into the Amundsen Sea sector. Wind variables are averaged annually within each box and correlated with site-specific precipitation. This dual-box approach captures both large-scale circulation (e.g., westerly flow surrounding the Amundsen Sea Low, ASL) and more localized synoptic variability relevant to upwelling of ocean water bodies into the Antarctic continental shelf and nearer to sensitive ice-shelf outlet regions of the Antarctic ice sheet. Correlation strength and significance ($p < 0.05$ threshold) are visualized using scaled markers.

To evaluate vertical atmospheric influences, we correlate annual site precipitation with ERA5 geopotential height anomalies at four pressure levels: mean sea level pressure (MSLP), 850 hPa, 500 hPa, and 200 hPa (z850, z500, z200). Geopotential height fields are spatially averaged over the Amundsen Sea box each year, and Pearson r and p-values are computed relative to local precipitation time series at each ice rise. This vertical framework allows us to assess the role of both surface and upper-level atmospheric circulation in modulating snowfall.

We then investigate oceanic and sea ice forcing of precipitation by analyzing ERA5-derived SST and SIC fields in the Amundsen Sea box. Annual mean SST and SIC are computed by spatially averaging the fields within the domain. Pearson correlations are calculated between each site's annual precipitation and the regional SST or SIC time series. This allows us to distinguish the effects of oceanic heat content and sea ice coverage on coastal moisture delivery (Holland & Kwok, 2012;

https://doi.org/10.5194/egusphere-2025-6010
Preprint. Discussion started: 17 December 2025
© Author(s) 2025. CC BY 4.0 License.

Schwanck et al., 2016). To facilitate comparison between oceanic and cryospheric controls, we compare SST-precipitation and SIC-precipitation correlations to highlight spatial differences in the magnitude and significance of each forcing, as well as to assess whether SST and SIC exert coherent or contrasting influences on local snowfall across the WAIS coast.

2.4 Large-Scale Climate Indices and Snowfall Correlations

To evaluate the influence of large-scale atmospheric and oceanic variability on precipitation across coastal West Antarctica, we reconstruct three key climate indices from ERA5 reanalysis fields: the Southern Annular Mode (SAM), Amundsen Sea Low (ASL), and Niño 3.4 (ENSO) indices. Each index is computed using annually averaged ERA5 single-variable fields (MSLP or SST) and then correlated with ERA5-derived annual precipitation at each of our 13 ice rises.

Following Marshall (2003), we calculate the SAM index as the difference in zonal-mean MSLP between mid-latitudes (40°S) and polar latitudes (65°S). This ERA5-derived SAM index closely matches Marshall (2003) (Figure B1). For each year, we average MSLP across all longitudes within these bands and subtract the polar average from the mid-latitude average. The resulting time series is then standardized (mean-zero, unit-variance). We compute Pearson correlation coefficients between this SAM index and the precipitation time series at each site, with significance assessed via corresponding p-values.

To represent variability in ASL strength, we average annual MSLP over the Amundsen Sea sector (60°–80°S, 170°W–62°W) and compute correlations between this calculated ASL (MSLP) and precipitation at each site. While Hosking et al. (2013) characterize the ASL using the relative central pressure of the low-pressure minimum, we find that regional MSLP averages better capture the relationship between synoptic-scale pressure variability and local precipitation at our coastal ice rise sites. This suggests that the spatial distribution of the pressure field, rather than just the intensity of the central low, is a key control on precipitation variability along the WAIS coast, consistent with recent findings emphasizing the importance of local atmospheric circulation patterns in this region (O'Connor et al., 2025). It also captures interannual shifts in the strength of the low-pressure anomaly over the Amundsen–Bellingshausen Seas.

Lastly, to quantify ENSO variability, we derive a Niño 3.4 index from ERA5 SST fields averaged over 5°S-5°N and 170°-120°W (Bamston et al., 1997; Trenberth, 1997). This ERA5-derived Niño 3.4 index also closely matches the values published by Trenberth et al. (2025) (B2). The resulting annual SST time series serves as our ENSO proxy, capturing both El Niño and La Niña phases. We again correlate this index with precipitation time series at each ice rise to assess tropical–polar teleconnections (Ding et al., 2011; Li et al., 2021). Together, these analyses provide a model-based assessment of how large-scale circulation modes influence precipitation at potential ice core sites along the WAIS coast. Future ice core records from these locations will allow validation of these reanalysis-derived climate relationships and enable reconstruction of these modes beyond the satellite era.

https://doi.org/10.5194/egusphere-2025-6010
Preprint. Discussion started: 17 December 2025
© Author(s) 2025. CC BY 4.0 License.

3 Results and Discussion

3.1 Reanalysis Datasets

3.1.1 Precipitation and Temperature Correlations

ERA5 data (1979-2022) show that the East Sector exhibits slightly warmer temperatures than the West Sector, with Noville Peninsula displaying the warmest and wettest annual average temperatures, while Bear Peninsula records the coldest and Sherman Island the driest (Table 2.1).

In the West Sector, Martin Peninsula experiences the coolest annual average temperatures and the highest average precipitation, while Siple Island is the warmest, and Guest Peninsula has the least precipitation. Seasonally, both sectors share similar trends: January is the warmest and driest month, while August is the coldest, and May is the wettest on average.

Ice Rise	Lat	Lon	Area (km2)	Max Height (m)	Avg. Ann Temp	Avg. Ann Precip	DJF Precip	MAM Precip	JJA Precip	SON Precip
Farwell	-72.84	-91.16	1,626.5	535	-12.6	0.99	15.9%	29.4%	28.5%	26.2%
Noville	-71.92	-98.60	1,093.9	494	-11.7	1.06	16.2%	29.4%	28.5%	25.9%
Sherman	-72.66	-99.79	1,193.6	489	-12.8	0.58	14.5%	29.5%	30.6%	25.4%
King	-73.08	-102.05	4,250.6	659	-12.6	0.63	13.1%	29.4%	31.9%	25.6%
Canisteo	-73.78	-102.14	1,721.7	630	-8.3	0.86	15.2%	28.0%	31.0%	25.8%
Bear	-74.55	-111.06	3,257.3	641	-13.2	0.98	15.1%	28.6%	29.9%	26.3%
Martin	-74.29	-114.29	3,202.3	655	-16.3	0.98	15.1%	29.0%	30.1%	25.8%
Wright	-74.05	-116.80	704.2	485	-14.4	0.89	14.3%	29.3%	31.2%	25.3%
Carney	-74.03	-121.81	5,101.1	647	-14.4	0.88	15.2%	29.2%	31.1%	24.5%
Siple	-73.98	-124.90	2,703.5	615	-13.7	0.89	16.4%	29.9%	29.8%	23.9%
Dean	-74.48	-127.65	699.3	397	-13.9	0.89	14.6%	29.9%	31.9%	23.5%
Guest	-76.32	-148.33	1,899.6	560	-16.2	0.67	19.7%	30.2%	28.5%	21.6%
Roosevelt	-79.33	-161.79	8,413.0	551	-26.2	0.14	19.8%	32.0%	28.9%	19.2%

Table 1: Key characteristics for each ice rise, including latitude, longitude, total area, maximum height (Bedmap2, Fretwell et al., 2013), average annual temperature (ERA5, 2 m), and total precipitation with seasonal distribution percentages (ERA5, surface level).

To assess consistency between reanalysis datasets used for Antarctic climate reconstruction, we compare ERA5 and MERRA-2 average temperature and precipitation data from 1979 to 2022 across our WAIS ice rise locations (Figure 3). While both datasets generally agree, important spatial and temporal discrepancies emerge. For precipitation, correlations between the two products are consistently high across all sites (Figure 3d), with coefficients ranging from 0.82 at Siple Island (SI) to 0.92 at Dean Island (DI). The spatial map (Figure 3e) confirms this strong agreement across West Antarctica. While high inter-product correlation suggests both reanalyses respond similarly to synoptic-scale forcing, it does not independently verify accuracy, as

https://doi.org/10.5194/egusphere-2025-6010
Preprint. Discussion started: 17 December 2025
© Author(s) 2025. CC BY 4.0 License.

both products could share similar biases. Future ice core records from these sites will provide observational constraints on reanalysis precipitation estimates.

In contrast, temperature correlations between reanalyses vary more widely, from 0.44 at Wright Island (WI) to 0.75 at Roosevelt Island (RI) (Figure 3a). This weaker agreement is evident in both the spatial correlation (Figure 3b) and in the time series (Figure 3c), where post-2005 MERRA-2 temperatures show a systematic cooling bias relative to ERA5. As Zhu et al. (2021) note, while MERRA-2 can capture monthly temperature variability over inland Antarctic stations, its correlations are generally lower than those of ERA5, possibly due to differences in sensor transitions and the dimensionality and input data of the assimilation systems used.

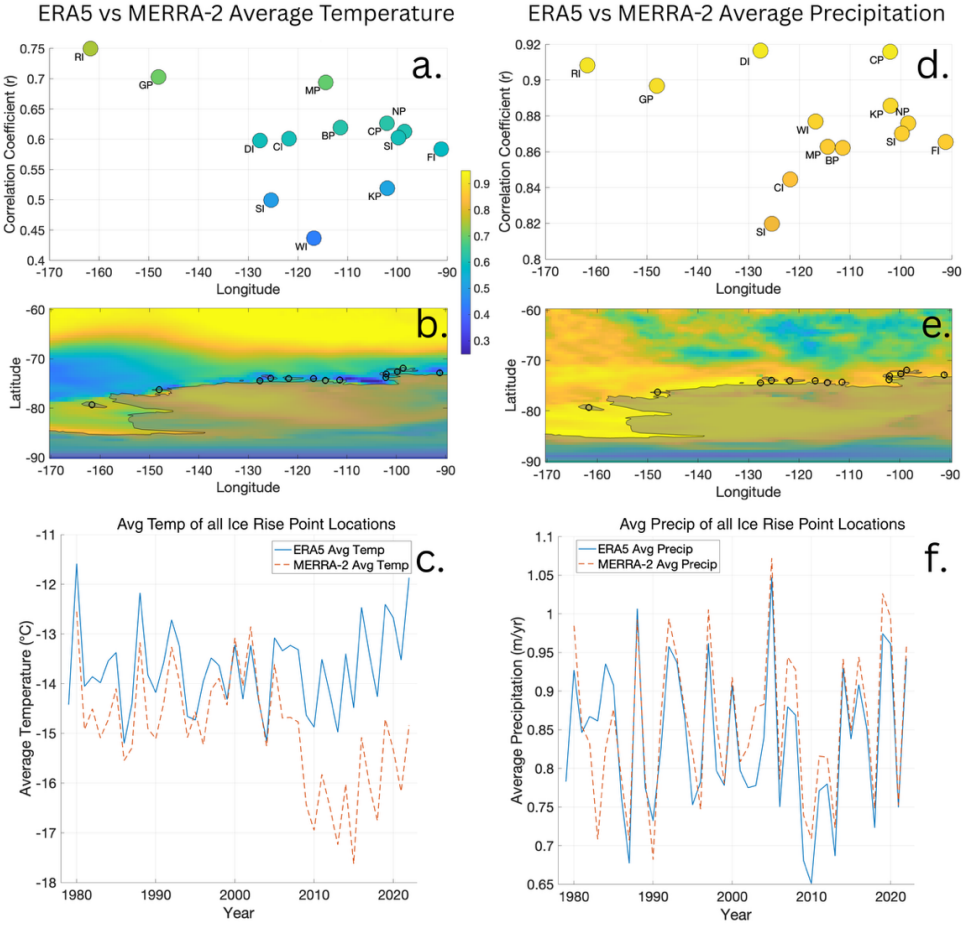

Figure 3: Correlation between ERA5 and MERRA-2 reanalysis datasets for temperature (panels a-c) and precipitation (panels d-f) at each ice rise for the 1979-2022 period. Panels a, b, d, and e show a correlation field visualized with a color-coded heatmap (higher correlation coefficients in yellow, lower coefficients in blue) and the 13 ice rise locations plotted. Statistical significance of the ERA5 and MERRA-2 comparison is indicated by marker size. Panels c and f average the temperature (c.) and precipitation (f.) for all the ice rise point locations annually for ERA5 (blue line) and MERRA-2 (dotted orange line).

https://doi.org/10.5194/egusphere-2025-6010
Preprint. Discussion started: 17 December 2025
© Author(s) 2025. CC BY 4.0 License.

Given the stronger consistency and better alignment with independent datasets, as well as its widespread use and evaluation in Antarctic climate studies (e.g. Bromwich et al., 2007, 2024), ERA5 is used for all subsequent analyses in this work. However, the inter-dataset differences, especially for temperature, highlight the ongoing challenges of using reanalysis in Antarctic climate studies and caution against over-interpreting absolute values or trends without observational validation, which is particularly challenging along the remote coastline of West Antarctica.

3.1.2 Wind Correlations

To evaluate the role of atmospheric circulation in driving precipitation variability at WAIS coastal ice rises, we correlate precipitation at each location with ERA5 10-meter surface winds: zonal wind (U-wind, east-west) and meridional wind (V-wind, north-south), averaged across the broader Amundsen Sea box (55°–72°S, 105°–150°W) and the narrower "Steig box" (72°–68°S, 125°–100°W) (Figure 4c, f). These analyses capture the influence of both broad-scale circulation regimes, such as the Southern Annular Mode (SAM), and more localized synoptic activity.

The zonal (U-wind) results over the Amundsen Sea box (Figure 4a) reveal a clear correlation dipole: West Sector ice rises (Roosevelt Island, Guest Peninsula, and Dean Island) exhibit statistically significant negative correlations with U-wind, while East Sector sites show only insignificant and slightly positive correlations. This result likely reflects the dominance of high-pressure systems during strong zonal wind regimes and broadly mirrors the influence of SAM. During positive SAM phases, westerly winds intensify and shift poleward (Marshall, 2003), promoting high-pressure ridging and subsidence over the WAIS coast. This increased atmospheric stability suppresses convection and decreases precipitation, consistent with the negative U-wind correlations observed in Figure 4a (Hosking et al., 2013; Marshall, 2003).

https://doi.org/10.5194/egusphere-2025-6010
Preprint. Discussion started: 17 December 2025
© Author(s) 2025. CC BY 4.0 License.

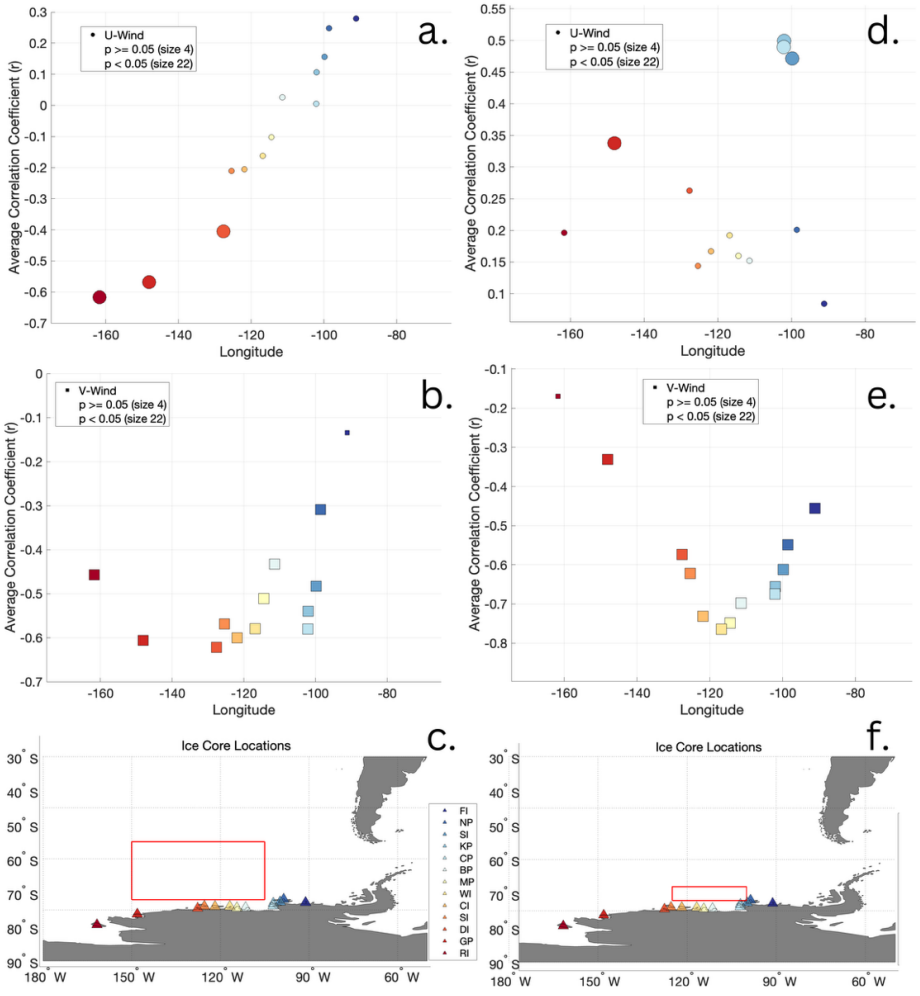

Figure 4: Correlation analysis between snowfall and zonal winds and meridional winds within a broad Amundsen Sea box and the Steig et al., 2012 coastal box. To reconstruct atmospheric conditions in a specific region (e.g., Amundsen Sea, CSB, Thwaites), focus on ice rises closest to it; to reconstruct broader zonal winds, focus on ice rises westward (Dean and Guest). To reconstruct Bellingshausen Sea pressure variability, focus on easterly ice rises.

The strength and spatial coherence of these negative U-wind–precipitation correlations across the West Sector, particularly at Guest Peninsula and Roosevelt Island, suggest that these sites are highly sensitive to changes in Southern Hemisphere westerly wind intensity and position. As such, they represent strong candidates for reconstructing past variability in zonal circulation regimes, including SAM-linked westerly wind behavior, an important signal in Antarctic paleoclimate records. Enhanced westerly winds may also influence local atmospheric stability, potentially suppressing vertical mixing and convection that would otherwise generate precipitation.

When U-wind is averaged over the more focused "Steig box" domain (Figure 4d), the pattern shifts and significant positive zonal correlations appear at East Sector ice rises nearest Pine Island Bay, including Canisteo Peninsula, where ice cores were collected as part of the Ross-Amundsen Ice Core Array (RAICA) initiative in January 2024 (Elliott, 2024). This reversal in

https://doi.org/10.5194/egusphere-2025-6010
Preprint. Discussion started: 17 December 2025
© Author(s) 2025. CC BY 4.0 License.

significance suggests that under more localized conditions, westerly flow in this narrower band may be associated with enhanced moisture delivery or lifting and precipitation. Additionally, during negative SAM phases, weakened and equatorward-shifted westerlies allow greater cyclonic intrusion and moisture delivery, which may also contribute to the positive U-wind-precipitation relationships observed at ice rises in the Pine Island region (Figure 4d).

Both West Sector and East Sector sites show negative correlations with meridional wind (V-wind, Figure 4b-e), indicating that stronger southerly flow (negative V) is linked to drier conditions, consistent with cold, dry air advection suppressing precipitation. Notably, Canisteo Peninsula, Bear Peninsula, Martin Peninsula, Wright Island, and Carney Island exhibit the strongest negative correlations, particularly when V-wind is averaged over the "Steig box," suggesting these sites may be especially sensitive to synoptically driven meridional flow.

This sensitivity to meridional winds has broader implications for understanding regional climate dynamics. Recent work by O'Connor et al. (2025) demonstrates that persistent northerly wind anomalies over the Amundsen Sea continental shelf are a key driver of ice shelf melting through their effects on coastal polynya formation and ocean heat transport. Their proxy reconstructions show significant northerly wind trends over the 20th century, highlighting meridional winds as an important component of regional climate variability with implications for outlet glaciers and ice shelves. The strong meridional wind sensitivity we observe at sites like Canisteo Peninsula and other East Sector ice rises positions these locations to potentially record this important atmospheric signal that influences both precipitation patterns and ice-ocean interactions.

We expanded on these interpretations by computing a SAM index based on the zonal mean sea-level pressure difference between 40°S and 65°S, following the method of Marshall (2003). The resulting SAM–precipitation correlation map (Figure 5) closely resembles the patterns seen in our U- and V-wind analyses, reinforcing the conclusion that SAM modulates wind–precipitation coupling, especially in the West Sector. However, as shown by Tsukernik and Lynch (2013), SAM alone cannot explain all meridional moisture transport variability, highlighting the role of transient synoptic systems and localized dynamics in shaping coastal West Antarctic accumulation.

https://doi.org/10.5194/egusphere-2025-6010
Preprint. Discussion started: 17 December 2025
© Author(s) 2025. CC BY 4.0 License.

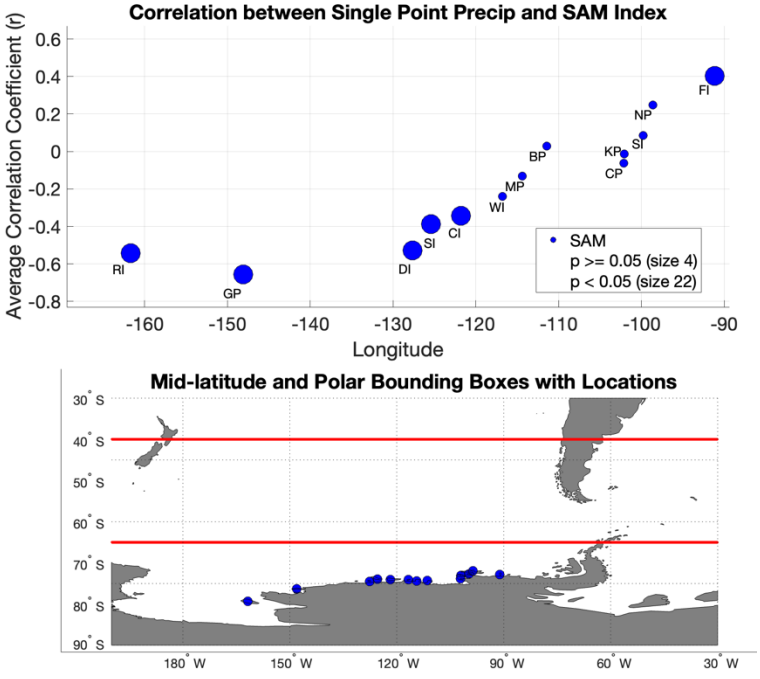

Figure 5: Correlation between precipitation at each ice rise and the Southern Annual Mode Index (Marshall, 2003). The index is defined by averaging MSLP across narrow latitude bands centered on −40° and −65° (red lines) and calculating the difference.

3.1.3 Geopotential Height Correlations

285 Geopotential height indices of the mean sea level pressure (MSL), z850, z500, and z200 reveal how atmospheric variability at different altitudes impacts local precipitation variability at WAIS ice rises. We average these variables over the Amundsen Sea box (72°S to 55°S and 150°W to 105°W) and find positive correlations between geopotential height at all levels and localized precipitation at ice rises in the West Sector (Figure 6).

https://doi.org/10.5194/egusphere-2025-6010
Preprint. Discussion started: 17 December 2025
© Author(s) 2025. CC BY 4.0 License.

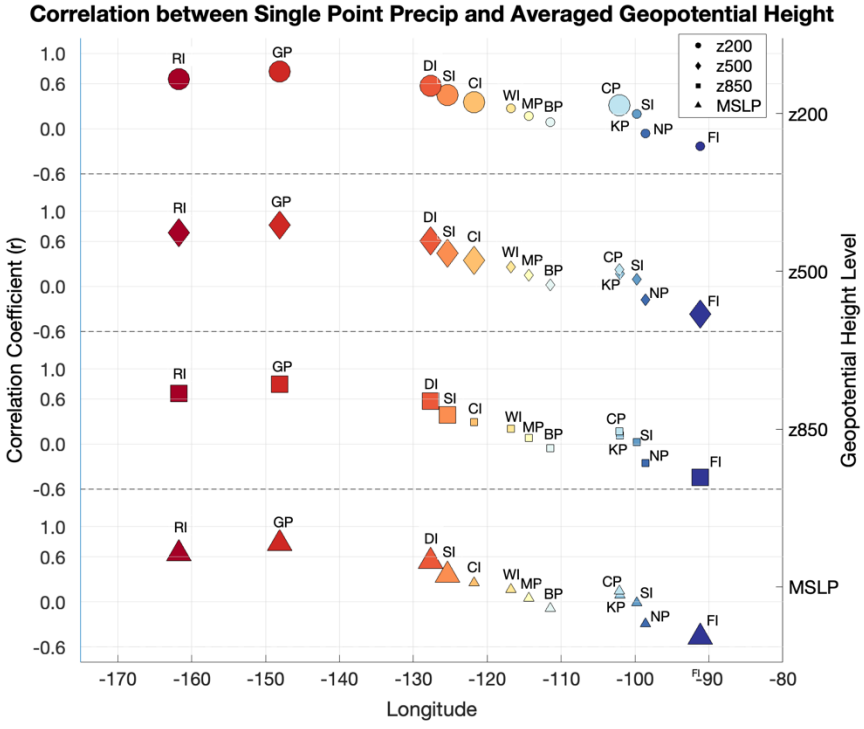

Figure 6: Correlation analysis between precipitation at individual ice rises (indicated by the color gradient from red to blue) and geopotential heights (indicated by shape: triangle is mean sea level pressure, square is z850, diamond is z500, and circle is z200) averaged across the broad Amundsen Sea box. Significant correlations ($p < 0.05$) are larger-sized markers.

This strong correlation between geopotential height and precipitation has been identified before, specifically while investigating Atmospheric River (AR) behavior in this region. Maclennan et al. (2023) found that high-pressure systems over the Antarctic Peninsula can act as blocking highs and prevent low-pressure systems and their associated moisture from moving away, similar to previous work (e.g. Emanuelsson et al., 2018). Blocking highs positioned over the Antarctic Peninsula, coupled with low-pressure systems in the Amundsen Sea Low region, redirect ARs to make landfall along the Amundsen Sea Embayment and Marie Byrd Land—the exact longitude of landfall is generally determined by the relative location of the pressure gradient. All surface-to-mid-troposphere correlations weaken the further east you travel along the coast towards the Bellingshausen Sea. However, Farwell Island, the easternmost ice rise, has a statistically significant negative correlation with MSLP, z850, and z500. This makes Farwell an intriguing location to reconstruct Bellingshausen Sea pressure variability. The negative correlation between these geopotential heights and precipitation at Farwell suggests that lower geopotential height anomalies are associated with increased precipitation in the Bellingshausen Sea region. We also analyzed MSLP correlations within the ASL index region (170° to 298° E, 80° to 60° S; geographic domain following Hosking et al., 2013) with precipitation at each ice rise (Figure 7). This regional MSLP average captures the broad pressure field variability associated with ASL activity. Here we see a similar trend to our Amundsen Sea box analysis, with statistically significant and higher

https://doi.org/10.5194/egusphere-2025-6010
Preprint. Discussion started: 17 December 2025
© Author(s) 2025. CC BY 4.0 License.

correlations along the West Sector and at Farwell Island, further supporting the importance of regional pressure variability for precipitation at these coastal sites.

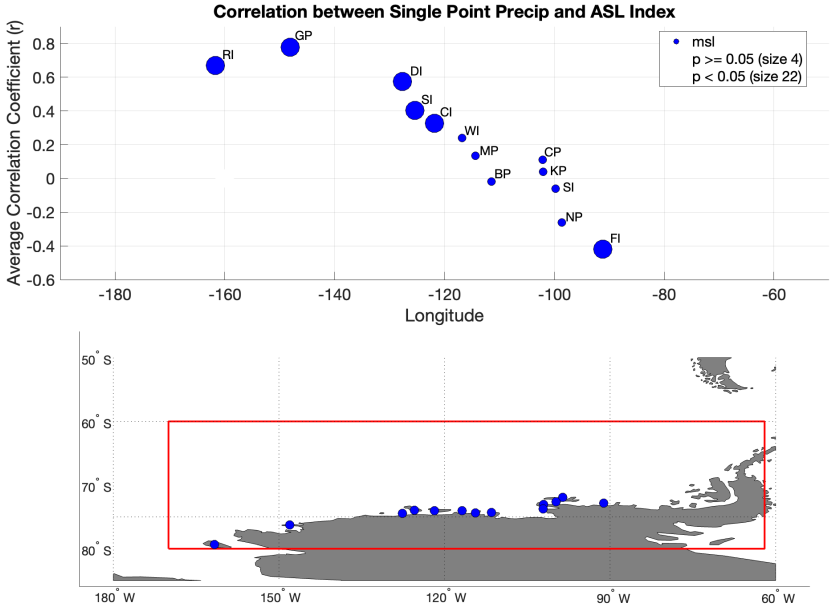

Figure 7: Correlation between precipitation at each ice rise and regional MSLP averaged over the Amundsen Sea Low index region (170° to 298° E, 80° to 60° S; Hosking et al., 2013). Marker size indicates statistical significance (p < 0.05 for larger markers).

3.1.4 Sea Surface Temperature Correlations

To assess the influence of Pacific Ocean variability on WAIS coastal precipitation, we examine correlations between snowfall and Niño 3.4 sea surface temperature (SST) anomalies in the central tropical Pacific. The Niño 3.4 region (5°N-5°S, 120°-170°W) is a widely used SST-based proxy for El Niño-Southern Oscillation (ENSO) variability, capturing oceanic thermal conditions that are closely linked to the coupled ocean-atmosphere processes defining ENSO, but alone it does not represent the full atmosphere-ocean index (Jones et al., 2014; Turner, 2004). SST anomalies in this region have been shown to modulate the strength and position of the Amundsen Sea Low (ASL), Southern Hemisphere westerly wind strength, and other aspects of West Antarctic climate via atmospheric teleconnections (Ding et al., 2011; Turner, 2004). Positive SST anomalies (La Niña) are typically associated with a deepened ASL, enhancing onshore moisture transport toward the WAIS coast. Conversely, negative anomalies (El Niño) weaken the ASL, reducing meridional flow and suppressing precipitation (Clem et al., 2016; Fogt et al., 2011). Our results show strong positive precipitation-SST correlations in the West Sector, particularly for the Roosevelt and Guest Peninsula sites (Figure 8). These relationships reflect the West Sector's dynamic connection to ASL variability and Pacific moisture sources.

https://doi.org/10.5194/egusphere-2025-6010
Preprint. Discussion started: 17 December 2025
© Author(s) 2025. CC BY 4.0 License.

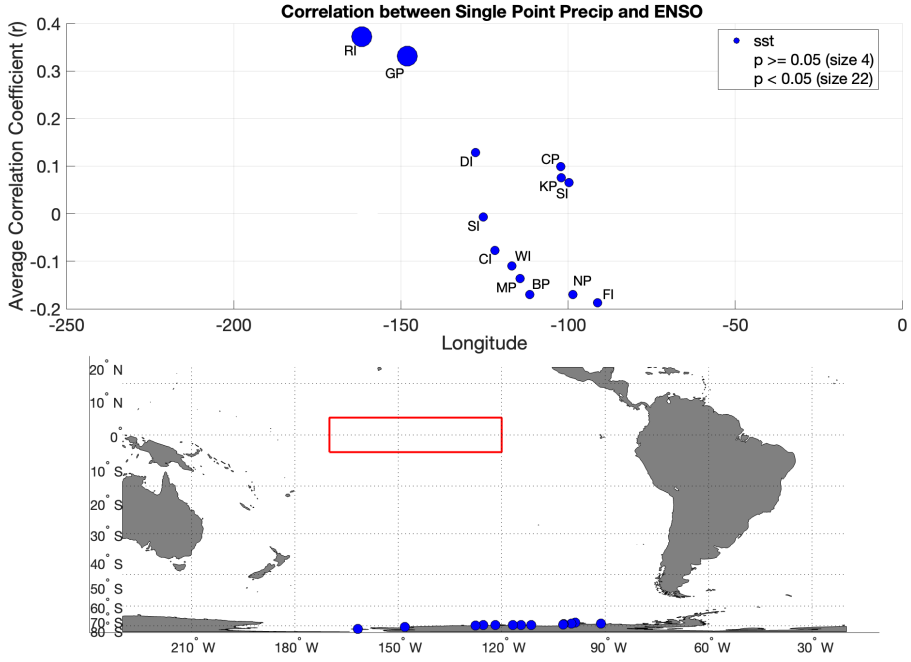

Figure 8: Correlation between precipitation at each ice rise and El Niño-Southern Oscillation. The index is defined by averaging SST across the ENSO box bounded by 5°N to 5°S and 120° to 170°W.

In contrast, ice rises in the East Sector exhibit weak and not statistically significant correlations with Niño 3.4 SST, suggesting more localized atmospheric processes dominate precipitation variability there (e.g., atmospheric pressure in the Bellingshausen Sea and relative position of high pressure with lows in the Amundsen Sea region) (Figure 8). This spatial pattern supports previous findings by Thomas et al. (2013), who showed that interannual variability at the Ferrigno (F10) ice core site (on the ice divide between the Ferrigno and Pine Island Glaciers in Ellsworth Land, West Antarctica, nearest to Farwell Island ice rise) was poorly correlated with ENSO indices. Instead, they linked precipitation variability to subtropical SST anomalies in the South Pacific Convergence Zone (SPCZ), consistent with different teleconnection mechanisms (Bromwich et al., 2013). Together, these results emphasize the heterogeneous influences of tropical Pacific Ocean SST on snowfall along the WAIS coast as seen in ERA5: large-scale ENSO-driven atmospheric circulation changes play a statistically significant role in modulating snowfall in the West Sector, while eastern sites are influenced by a more complex combination of processes, possibly including subtropical interactions outside the canonical tropical ENSO framework.

3.1.5 Sea Ice Concentrations

Sea ice concentration (SIC) variability along the WAIS coast serves as an indicator of large-scale atmospheric circulation, particularly SAM, ENSO, and the Atlantic Multidecadal Oscillation (AMO), which also modulate precipitation and surface conditions across seasonal to decadal timescales (Kohyama & Hartmann, 2016). SIC is also shaped by wind-driven dynamic transport, atmospheric thermal advection, and oceanic currents (Holland & Kwok, 2012; Schwanck et al., 2016). Coastal ice

https://doi.org/10.5194/egusphere-2025-6010
Preprint. Discussion started: 17 December 2025
© Author(s) 2025. CC BY 4.0 License.

rises themselves can also influence local sea ice distributions by altering wind flow, sometimes supporting coastal polynyas on their western flanks and multi-year land-fast ice on the eastern side (Matsuoka et al., 2015).

To assess the relationship between sea ice and WAIS ice rise snowfall, we correlate 1979-2022 averaged ERA5 SIC with precipitation at each of the 13 ice rise locations. SIC values are averaged over a bounding box spanning the eastern Amundsen Sea sector (72–68°S, 125–100°W), consistent with the domain used for wind and SST analyses (Section 2.3). We find that ice rises in the West Sector exhibit strong, statistically significant negative correlations between precipitation and SIC, particularly near Guest Peninsula, the westernmost WAIS ice rise located at the northern margin of Sulzberger Ice Shelf near the Ford Ranges. In contrast, East Sector sites such as Noville and Farwell ice rises show weak or insignificant correlations. This spatial pattern again highlights the West Sector's stronger coupling to synoptic-scale atmospheric dynamics, especially the Amundsen Sea Low (ASL), which governs much of the heat and moisture advection into the region. The similarity between SIC–precipitation correlations and wind field patterns (Section 3.1.2) underscores the interconnectedness of ocean–atmosphere processes in this region.

In particular, the ice rises in the West Sector offer a strong observational window into regional sea ice variability. For example, Dean Island shows a pronounced negative correlation between local precipitation and sea ice concentration immediately offshore in the Amundsen Sea (Figure 9b), indicating that ice core–derived precipitation variability may capture dynamic interactions between the ocean–atmosphere system. In contrast, sites in the East Sector, such as King Peninsula, show much weaker and more spatially diffuse correlations with SIC (Figure 9a), suggesting limited coupling between local accumulation and sea ice anomalies in that region. This spatial gradient highlights the potential for more reliable sea ice reconstructions from West Sector ice rise ice core sites, where precipitation is more directly modulated by atmospheric circulation patterns like the ASL, and where regional sea ice is more sensitive to variability in wind and heat transport.

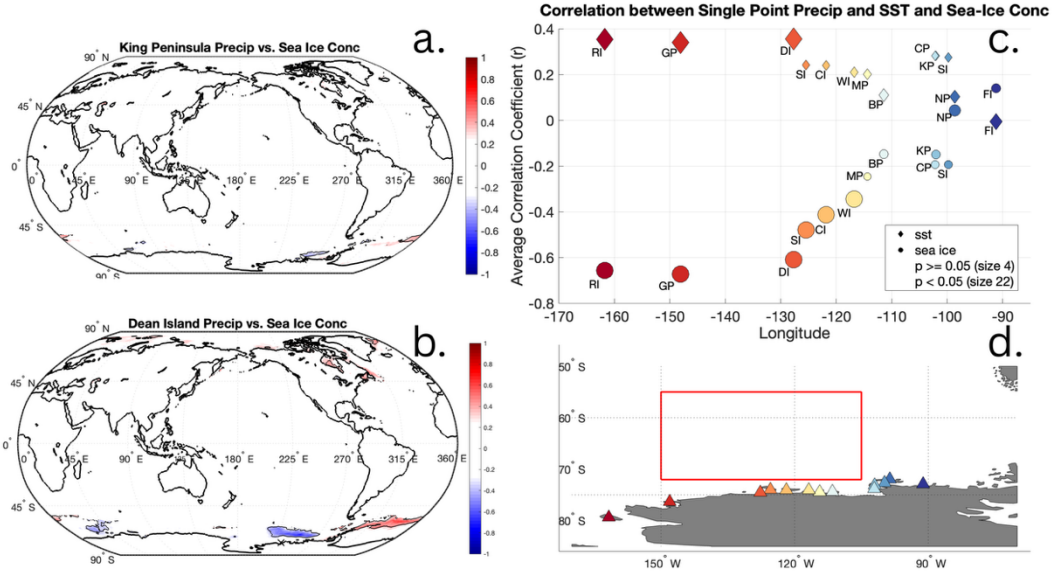

https://doi.org/10.5194/egusphere-2025-6010
Preprint. Discussion started: 17 December 2025
© Author(s) 2025. CC BY 4.0 License.

Figure 9: Sea surface temperature and sea ice concentration comparison. Panels a and b: correlation between precipitation at each ice rise and global sea ice concentration at King Peninsula (a) and Dean Island (b). Panel c: correlation between precipitation at each ice rise and sea surface temperature (SST, diamond) as well as sea ice concentration (SIC, circle) averaged over the Amundsen box.

Contrastingly, precipitation covaries positively with sea surface temperatures (SST) in the same Amundsen Sea box (Figures 9c and 9d). Higher SSTs here are associated with increased precipitation and decreased SIC, reflecting possible enhanced ocean–atmosphere coupling, when warmer ocean surfaces promote atmospheric instability, increased evaporation, and moisture flux toward the WAIS coast (Steig et al., 2012). Lower SSTs, on the other hand, are caused by more stable conditions with colder and weaker ocean-atmosphere coupling, suppressed precipitation, and increased SIC.

4 Conclusion

Coastal ice rises along the West Antarctic Ice Sheet (WAIS) are ideal locations to record key climate variability driven by dynamic ice, ocean, and atmosphere interactions. From glaciological and climatological perspectives, their preservation of high snow accumulation rates and exposure to marine and atmospheric influences make ice rises valuable sites for future ice core drilling and paleoclimate reconstruction (Steig and Neff, 2018; Neff, 2020). Despite the scarcity of direct ground observations at WAIS ice rises, this study leverages ERA5 and MERRA-2 reanalysis datasets to assess the climate drivers of precipitation variability across the WAIS coast from 1979 to 2022.

Our results demonstrate that interannual snowfall variability at these sites is strongly influenced by major climate drivers and indices, including ENSO, SAM, ASL, and regional wind fields. SAM and ENSO modulate both zonal (U-wind) and meridional (V-wind) circulation patterns across the Amundsen Sea sector, and these in turn control moisture delivery and precipitation. For instance, SAM–precipitation correlations extend across nearly all West Sector sites, from Roosevelt Island to Carney Island, highlighting their potential to reconstruct Southern Hemisphere westerly wind variability. Additionally, strong and consistent negative correlations with V-wind across all sites demonstrate that each ice rise is sensitive to meridional flow from the north, the primary direction of moisture transport.

Looking at how these correlations evolve across the coast, clear spatial distinctions emerge between West and East Sector ice rises. In the West Sector, sites such as Roosevelt Island, Guest Peninsula, and Dean Island exhibit strong positive correlations between precipitation and SST, and strong negative correlations with SIC, reflecting a dynamic feedback in which reduced sea ice and warmer ocean surfaces enhance atmospheric moisture availability and snowfall. These sites also exhibit strong negative correlations with U-wind in the broader Amundsen Sea box, consistent with the influence of SAM and ASL-driven subsidence during periods of strong westerlies. Guest Peninsula shows especially strong precipitation–SIC and wind relationships, suggesting strong potential for reconstructing broader circulation regimes, including the Southern Hemisphere westerlies and Amundsen Sea conditions. This finding represents a significant step toward developing paleoclimate records of broad-scale westerly wind behavior, a key component of Antarctic climate variability.

On the East Sector, Canisteo Peninsula and neighboring ice rises in the Pine Island Bay region show significant positive correlations between U-wind and precipitation when averaged over the Steig box—a region chosen for its possible significance

https://doi.org/10.5194/egusphere-2025-6010
Preprint. Discussion started: 17 December 2025
© Author(s) 2025. CC BY 4.0 License.

in wind-driven advection of CDW onto the Antarctic continental shelf. This contrasts with the more common negative correlations westward and suggests that these sites are uniquely positioned to record zonal wind variability at Thwaites and Pine Island glaciers within this narrower sector. These Pine Island Bay ice rises also exhibit strong sensitivity to meridional winds, which recent work has identified as important drivers of regional ice-ocean interactions (O'Connor et al., 2025), highlighting the value of recently collected ice cores at Canisteo Peninsula (Neff, unpublished). This dual sensitivity to both zonal and meridional wind variability positions these sites as particularly valuable for reconstructing the atmospheric conditions that influence precipitation patterns as well as broader ice sheet dynamics in this critical region. Further east, Farwell Island stands out for its significant negative correlation with 500 hPa geopotential height, indicating sensitivity to Bellingshausen Sea pressure variability, a key regional pressure system affecting snowfall. Unlike West Sector sites, East Sector ice rises show weaker connections to ENSO and SST/SIC, suggesting a stronger influence from localized synoptic-scale pressure and wind variability.

Taken together, these results confirm that WAIS coastal ice rises serve as spatially distributed, climatically sensitive archives. Their relationships with westerly winds, meridional moisture transport, sea ice extent, and geopotential height anomalies strengthen the value of a multi-site approach. Future ice core records from these ice rises hold significant potential for reconstructing past variability in ocean-atmosphere circulation relevant to the broader Amundsen Sea sector and the stability of outlet glaciers such as Pine Island and Thwaites.

Data availability

All raw data can be provided by the corresponding authors upon request.

Author contributions

J. R. Andreasen and P. D. Neff planned the research; J. R. Andreasen performed the measurements; J. R. Andreasen and P. D. Neff analyzed the data, wrote the manuscript draft, and reviewed and edited the manuscript.

Competing interests

The authors declare that they have no conflict of interest.

Acknowledgements

This work was led by J. R. Andreasen while at the University of Minnesota's Department of Soil, Water, and Climate. The authors gratefully acknowledge the European Centre for Medium-Range Weather Forecasts (ECMWF) for producing the ERA5 reanalysis dataset, made available through the Copernicus Climate Data Store, as well as NASA's Global Modeling and

https://doi.org/10.5194/egusphere-2025-6010
Preprint. Discussion started: 17 December 2025
© Author(s) 2025. CC BY 4.0 License.

Assimilation Office (GMAO) for producing the MERRA-2 reanalysis dataset. We also acknowledge the field and logistical support provided through the Ross–Amundsen Ice Core Array (RAICA) initiative, which facilitated ice-core recovery at the Canisteo Peninsula and contributed to the broader research context motivating this study. Lastly, we acknowledge the use of institutional computing resources at the University of Minnesota, as well as the broader research infrastructure supporting reanalysis production and distribution.

Financial Support

J. R. Andreasen was supported by the NASA Future Investigators in NASA Earth and Space Science and Technology (FINESST) Award (grant no. 80NSSC21K1615). J. R. Andreasen and P. D. Neff were supported by the RAICA project (I-345-M) through NSF Office of Polar Programs Award 2304836.

https://doi.org/10.5194/egusphere-2025-6010
Preprint. Discussion started: 17 December 2025
© Author(s) 2025. CC BY 4.0 License.

Appendix A: Conceptual Schematics of SAM and ENSO Impacts on West Antarctica

435

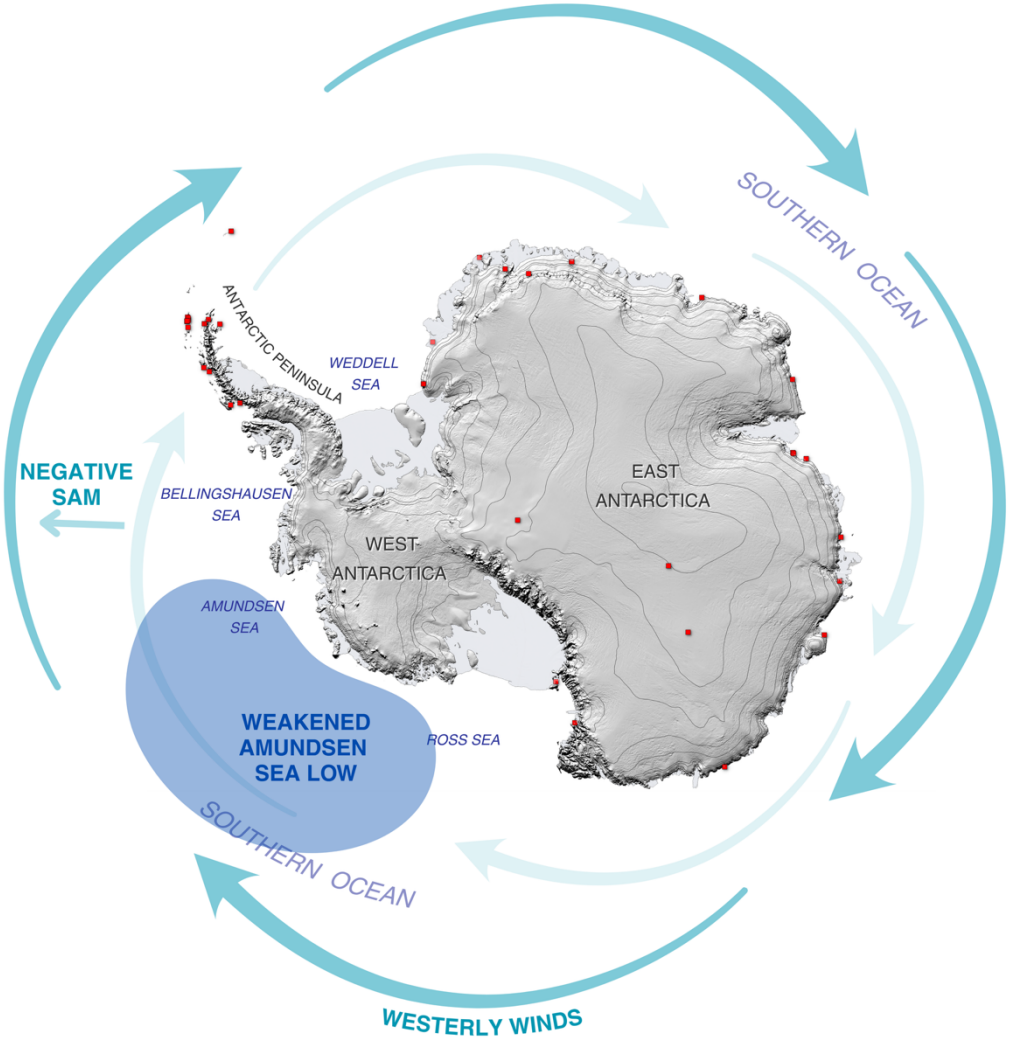

Figure A1: Negative SAM, weakens and shifts westerly winds away from Antarctica, weakening the Amundsen Sea Low. This reduces moisture transport and snowfall to the ice sheet.

https://doi.org/10.5194/egusphere-2025-6010
Preprint. Discussion started: 17 December 2025
© Author(s) 2025. CC BY 4.0 License.

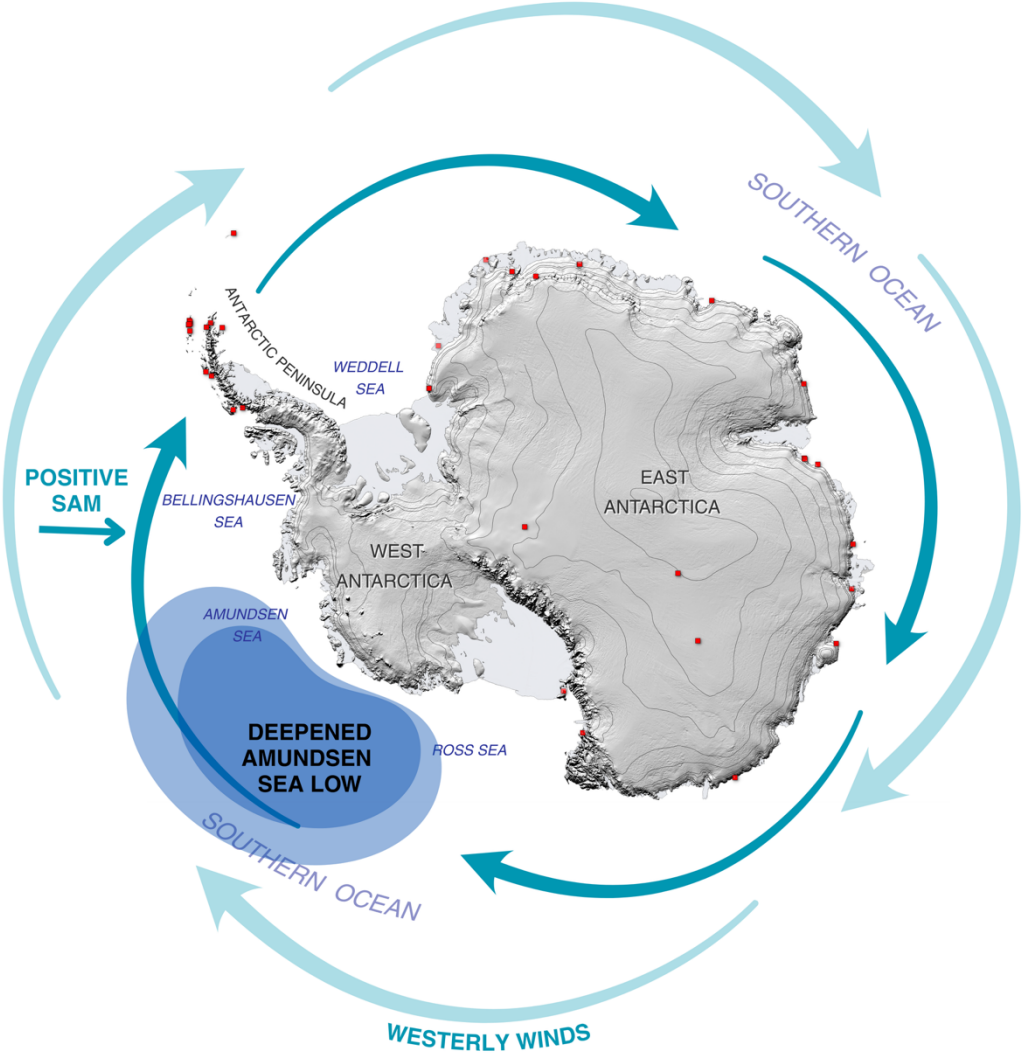

Figure A2: Positive SAM, strengthens and shifts westerly winds closer to Antarctica, deepening the Amundsen Sea Low. This can increase storm frequency along some coasts but cause high-pressure ridging and reduced moisture in others, depending on location.

https://doi.org/10.5194/egusphere-2025-6010
Preprint. Discussion started: 17 December 2025
© Author(s) 2025. CC BY 4.0 License.

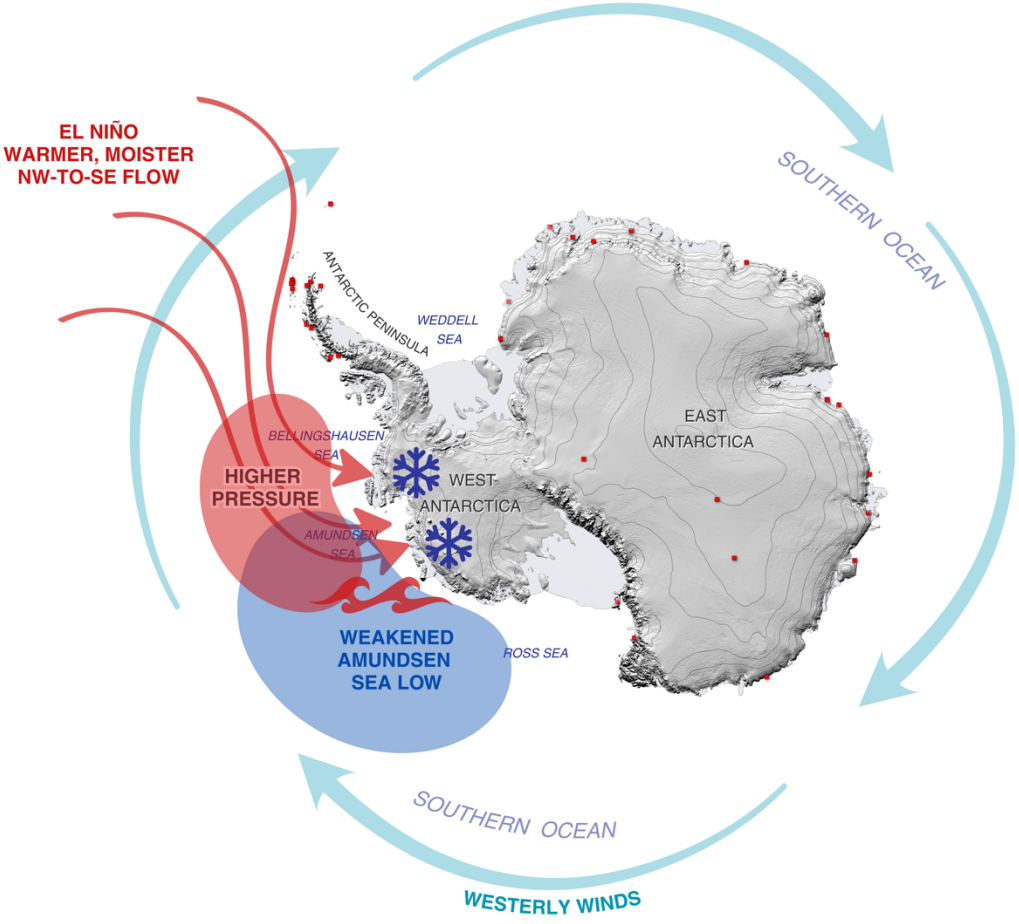

Figure A3: El Niño phase of ENSO, when warm tropical Pacific waters weaken the Amundsen Sea Low, forming a higher pressure center. This shift drives NW–SE winds that carry warm, moist air to West Antarctica, boosting snowfall and drive upwelling of warm Circumpolar Deep Water.

https://doi.org/10.5194/egusphere-2025-6010
Preprint. Discussion started: 17 December 2025
© Author(s) 2025. CC BY 4.0 License.

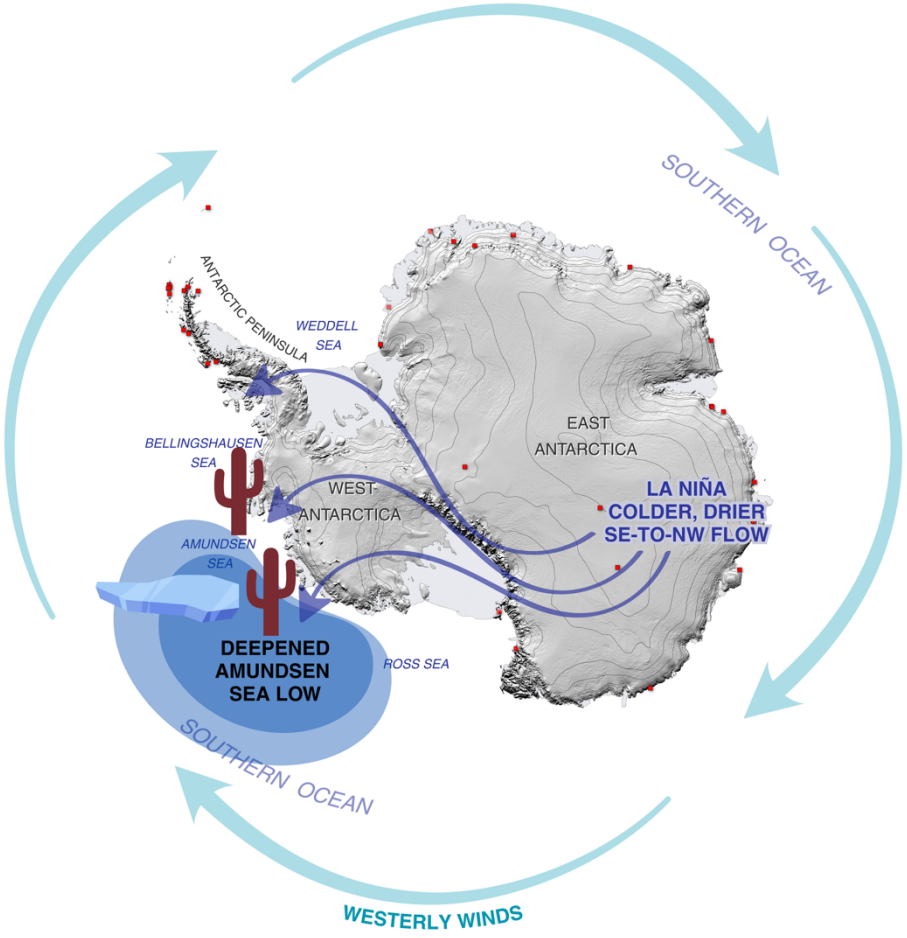

Figure A4: La Niña phase of ENSO, when cool tropical Pacific temperatures strengthen the Amundsen Sea Low, deepening the low-pressure center. This drives SE–NW winds that bring cold, dry air from the interior, reducing snowfall, and weakens upwelling of warm Circumpolar Deep Water, limiting basal melt and promoting sea ice growth.

https://doi.org/10.5194/egusphere-2025-6010
Preprint. Discussion started: 17 December 2025
© Author(s) 2025. CC BY 4.0 License.

Appendix B: Validation of ERA5-Derived SAM and Niño 3.4 Indices

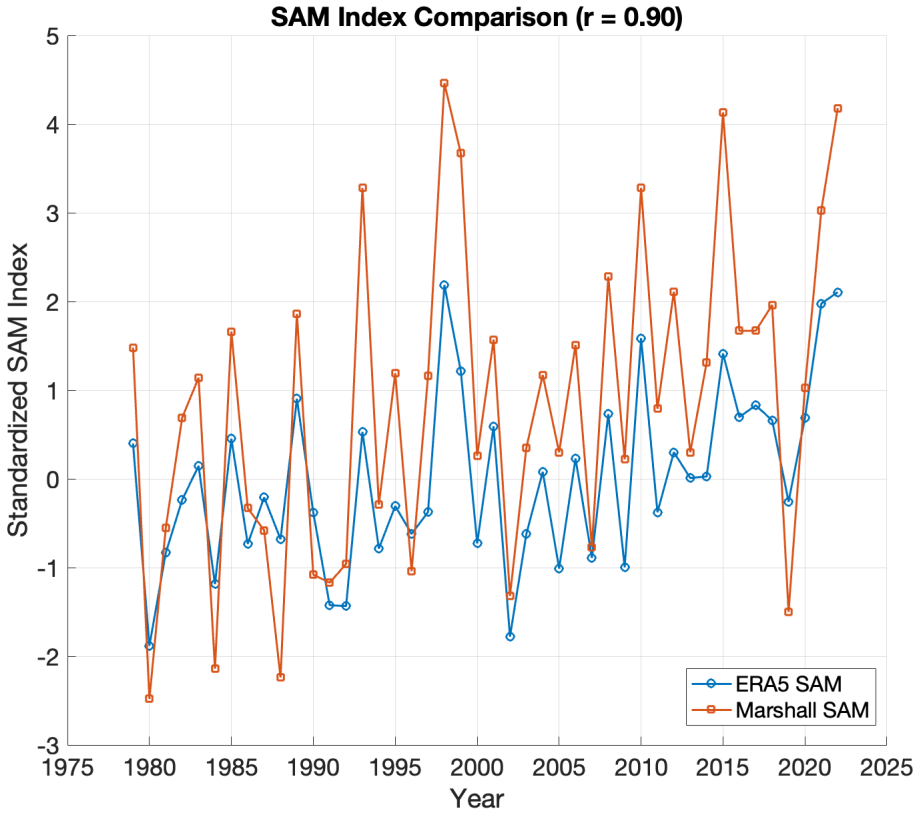

Figure B1: Comparison of standardized SAM index values, ERA5-derived SAM vs. Marshall et al. (2003) calculated SAM.

https://doi.org/10.5194/egusphere-2025-6010
Preprint. Discussion started: 17 December 2025
© Author(s) 2025. CC BY 4.0 License.

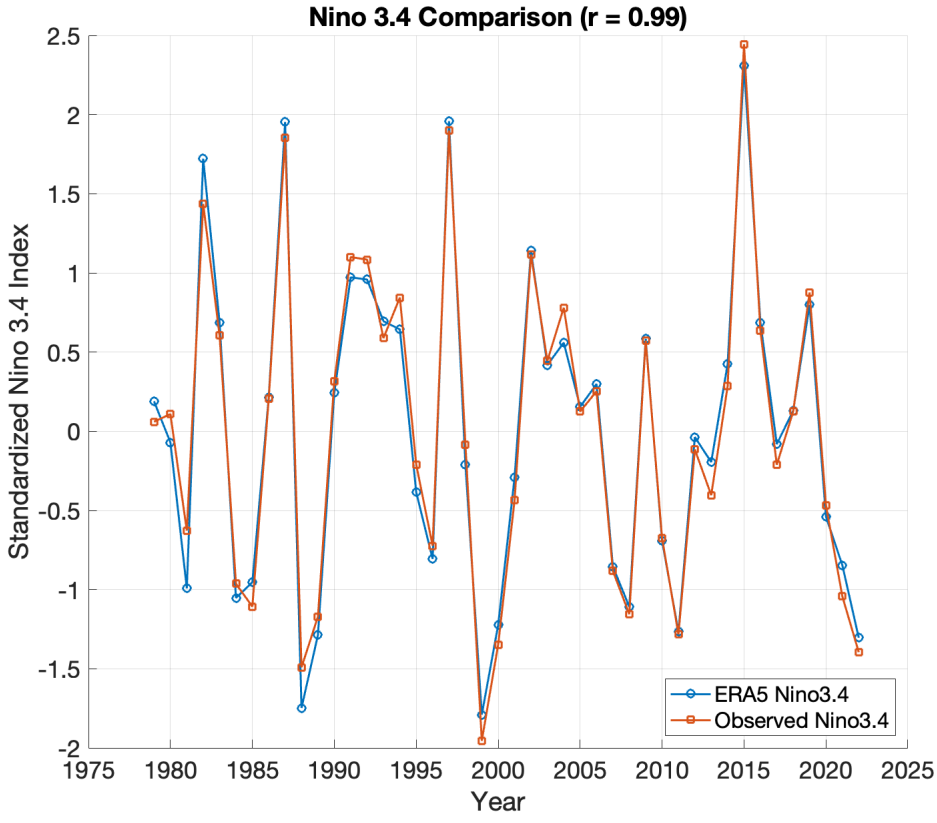

Figure B2: Comparison of standardized Niño 3.4 index values, ERA5-derived Niño 3.4 vs. Trenberth et al. (2025) observed Niño 3.4.

References

Assmann, K. M., Hellmer, H. H., and Jacobs, S. S.: Amundsen Sea ice production and transport, J. Geophys. Res., 110, https://doi.org/10.1029/2004jc002797, 2005.

Bamber, J. L., Riva, R. E. M., Vermeersen, B. L. A., and LeBrocq, A. M.: Reassessment of the Potential Sea-Level Rise from a Collapse of the West Antarctic Ice Sheet, Science, 324, 901–903, https://doi.org/10.1126/science.1169335, 2009.

Bamston, A. G., Chelliah, M., and Goldenberg, S. B.: Documentation of a highly ENSO-related sst region in the equatorial pacific: Research note, Atmosphere-Ocean, 35, 367–383, https://doi.org/10.1080/07055900.1997.9649597, 1997.

Banta, J. R., McConnell, J. R., Frey, M. M., Bales, R. C., and Taylor, K.: Spatial and temporal variability in snow accumulation at the West Antarctic Ice Sheet Divide over recent centuries, J. Geophys. Res., 113, https://doi.org/10.1029/2008jd010235, 2008.

https://doi.org/10.5194/egusphere-2025-6010
Preprint. Discussion started: 17 December 2025
© Author(s) 2025. CC BY 4.0 License.

Barr, I. D. and Lovell, H.: A review of topographic controls on moraine distribution, Geomorphology, 226, 44–64, https://doi.org/10.1016/j.geomorph.2014.07.030, 2014.

Bindschadler, R., Vornberger, P., Fleming, A., Fox, A., Mullins, J., Binnie, D., Paulsen, S., Granneman, B., and Gorodetzky, D.: The Landsat Image Mosaic of Antarctica, Remote Sensing of Environment, 112, 4214–4226, https://doi.org/10.1016/j.rse.2008.07.006, 2008.

Bromwich, D. H., Fogt, R. L., Hodges, K. I., and Walsh, J. E.: A tropospheric assessment of the ERA-40, NCEP, and JRA-25 global reanalyses in the polar regions, J. Geophys. Res., 112, 2006JD007859, https://doi.org/10.1029/2006JD007859, 2007.

Bromwich, D. H., Nicolas, J. P., Monaghan, A. J., Lazzara, M. A., Keller, L. M., Weidner, G. A., and Wilson, A. B.: Central West Antarctica among the most rapidly warming regions on Earth, Nature Geosci, 6, 139–145, https://doi.org/10.1038/ngeo1671, 2013.

Bromwich, D. H., Ensign, A., Wang, S., and Zou, X.: Major Artifacts in ERA5 2-m Air Temperature Trends Over Antarctica Prior to and During the Modern Satellite Era, Geophysical Research Letters, 51, https://doi.org/10.1029/2024gl111907, 2024.

Clem, K. R., Renwick, J. A., McGregor, J., and Fogt, R. L.: The relative influence of ENSO and SAM on Antarctic Peninsula climate, JGR Atmospheres, 121, 9324–9341, https://doi.org/10.1002/2016jd025305, 2016.

Cook, A. J., Holland, P. R., Meredith, M. P., Murray, T., Luckman, A., and Vaughan, D. G.: Ocean forcing of glacier retreat in the western Antarctic Peninsula, Science, 353, 283–286, https://doi.org/10.1126/science.aae0017, 2016.

Criscitiello, A. S., Das, S. B., Karnauskas, K. B., Evans, M. J., Frey, K. E., Joughin, I., Steig, E. J., McConnell, J. R., and Medley, B.: Tropical Pacific Influence on the Source and Transport of Marine Aerosols to West Antarctica*, Journal of Climate, 27, 1343–1363, https://doi.org/10.1175/jcli-d-13-00148.1, 2014.

Dalaiden, Q., Goosse, H., Rezsöhazy, J., and Thomas, E. R.: Reconstructing atmospheric circulation and sea-ice extent in the West Antarctic over the past 200 years using data assimilation, Clim Dyn, 57, 3479–3503, https://doi.org/10.1007/s00382-021-05879-6, 2021.

Dansgaard, W., Johnsen, S. J., Møller, J., and Langway, C. C.: One Thousand Centuries of Climatic Record from Camp Century on the Greenland Ice Sheet, Science, 166, 377–381, https://doi.org/10.1126/science.166.3903.377, 1969.

Ding, Q., Steig, E. J., Battisti, D. S., and Küttel, M.: Winter warming in West Antarctica caused by central tropical Pacific warming, Nature Geosci, 4, 398–403, https://doi.org/10.1038/ngeo1129, 2011.

Dutrieux, P., De Rydt, J., Jenkins, A., Holland, P. R., Ha, H. K., Lee, S. H., Steig, E. J., Ding, Q., Abrahamsen, E. P., and Schröder, M.: Strong Sensitivity of Pine Island Ice-Shelf Melting to Climatic Variability, Science, 343, 174–178, https://doi.org/10.1126/science.1244341, 2014.

Elliott, C.: Drilling on the edge, Science, 384, 262–266, https://doi.org/10.1126/science.ziof373, 2024.

Emanuelsson, B. D., Bertler, N. A. N., Neff, P. D., Renwick, J. A., Markle, B. R., Baisden, W. T., and Keller, E. D.: The role of Amundsen–Bellingshausen Sea anticyclonic circulation in forcing marine air intrusions into West Antarctica, Clim Dyn, 51, 3579–3596, https://doi.org/10.1007/s00382-018-4097-3, 2018.

https://doi.org/10.5194/egusphere-2025-6010
Preprint. Discussion started: 17 December 2025
© Author(s) 2025. CC BY 4.0 License.

Fogt, R. L., Bromwich, D. H., and Hines, K. M.: Understanding the SAM influence on the South Pacific ENSO teleconnection, Clim Dyn, 36, 1555–1576, https://doi.org/10.1007/s00382-010-0905-0, 2011.

Fretwell, P., Pritchard, H. D., Vaughan, D. G., Bamber, J. L., Barrand, N. E., Bell, R., Bianchi, C., Bingham, R. G., Blankenship, D. D., Casassa, G., Catania, G., Callens, D., Conway, H., Cook, A. J., Corr, H. F. J., Damaske, D., Damm, V., Ferraccioli, F., Forsberg, R., Fujita, S., Gim, Y., Gogineni, P., Griggs, J. A., Hindmarsh, R. C. A., Holmlund, P., Holt, J. W., Jacobel, R. W., Jenkins, A., Jokat, W., Jordan, T., King, E. C., Kohler, J., Krabill, W., Riger-Kusk, M., Langley, K. A., Leitchenkov, G., Leuschen, C., Luyendyk, B. P., Matsuoka, K., Mouginot, J., Nitsche, F. O., Nogi, Y., Nost, O. A., Popov, S. V., Rignot, E., Rippin, D. M., Rivera, A., Roberts, J., Ross, N., Siegert, M. J., Smith, A. M., Steinhage, D., Studinger, M., Sun, B., Tinto, B. K., Welch, B. C., Wilson, D., Young, D. A., Xiangbin, C., and Zirizzotti, A.: Bedmap2: improved ice bed, surface and thickness datasets for Antarctica, The Cryosphere, 7, 375–393, https://doi.org/10.5194/tc-7-375-2013, 2013.

Holland, P. R. and Kwok, R.: Wind-driven trends in Antarctic sea-ice drift, Nature Geosci, 5, 872–875, https://doi.org/10.1038/ngeo1627, 2012.

Hosking, J. S., Orr, A., Marshall, G. J., Turner, J., and Phillips, T.: The Influence of the Amundsen–Bellingshausen Seas Low on the Climate of West Antarctica and Its Representation in Coupled Climate Model Simulations, Journal of Climate, 26, 6633–6648, https://doi.org/10.1175/JCLI-D-12-00813.1, 2013.

Hosking, J. S., Orr, A., Bracegirdle, T. J., and Turner, J.: Future circulation changes off West Antarctica: Sensitivity of the Amundsen Sea Low to projected anthropogenic forcing, Geophysical Research Letters, 43, 367–376, https://doi.org/10.1002/2015gl067143, 2016.

Jones, T. R., White, J. W. C., and Popp, T.: Siple Dome shallow ice cores: a study in coastal dome microclimatology, Clim. Past, 10, 1253–1267, https://doi.org/10.5194/cp-10-1253-2014, 2014.

Joughin, I. and Alley, R. B.: Stability of the West Antarctic ice sheet in a warming world, Nature Geosci, 4, 506–513, https://doi.org/10.1038/ngeo1194, 2011.

Joughin, I., Smith, B. E., and Medley, B.: Marine Ice Sheet Collapse Potentially Under Way for the Thwaites Glacier Basin, West Antarctica, Science, 344, 735–738, https://doi.org/10.1126/science.1249055, 2014.

Karoly, D. J.: Southern Hemisphere Circulation Features Associated with El Niño-Southern Oscillation Events, J. Climate, 2, 1239–1252, https://doi.org/10.1175/1520-0442(1989)002%253C1239:SHCFAW%253E2.0.CO;2, 1989.

Kaspari, S., Mayewski, P. A., Dixon, D. A., Spikes, V. B., Sneed, S. B., Handley, M. J., and Hamilton, G. S.: Climate variability in West Antarctica derived from annual accumulation-rate records from ITASE firn/ice cores, Ann. Glaciol., 39, 585–594, https://doi.org/10.3189/172756404781814447, 2004.

Kohyama, T. and Hartmann, D. L.: Antarctic Sea Ice Response to Weather and Climate Modes of Variability*, Journal of Climate, 29, 721–741, https://doi.org/10.1175/jcli-d-15-0301.1, 2016.

Lee, D. Y., Petersen, M. R., and Lin, W.: The Southern Annular Mode and Southern Ocean Surface Westerly Winds in E3SM, Earth and Space Science, 6, 2624–2643, https://doi.org/10.1029/2019EA000663, 2019.

https://doi.org/10.5194/egusphere-2025-6010
Preprint. Discussion started: 17 December 2025
© Author(s) 2025. CC BY 4.0 License.

Li, X., Cai, W., Meehl, G. A., Chen, D., Yuan, X., Raphael, M., Holland, D. M., Ding, Q., Fogt, R. L., Markle, B. R., Wang, G., Bromwich, D. H., Turner, J., Xie, S.-P., Steig, E. J., Gille, S. T., Xiao, C., Wu, B., Lazzara, M. A., Chen, X., Stammerjohn, S., Holland, P. R., Holland, M. M., Cheng, X., Price, S. F., Wang, Z., Bitz, C. M., Shi, J., Gerber, E. P., Liang, X., Goosse, H., Yoo, C., Ding, M., Geng, L., Xin, M., Li, C., Dou, T., Liu, C., Sun, W., Wang, X., and Song, C.: Tropical teleconnection impacts on Antarctic climate changes, Nat Rev Earth Environ, 2, 680–698, https://doi.org/10.1038/s43017-021-00204-5, 2021.

Maclennan, M. L., Lenaerts, J. T. M., Shields, C. A., Hoffman, A. O., Wever, N., Thompson-Munson, M., Winters, A. C., Pettit, E. C., Scambos, T. A., and Wille, J. D.: Climatology and surface impacts of atmospheric rivers on West Antarctica, The Cryosphere, 17, 865–881, https://doi.org/10.5194/tc-17-865-2023, 2023.

Marshall, G. J.: Trends in the Southern Annular Mode from Observations and Reanalyses, J. Climate, 16, 4134–4143, https://doi.org/10.1175/1520-0442(2003)016%253C4134:TITSAM%253E2.0.CO;2, 2003.

Matsuoka, K., Hindmarsh, R. C. A., Moholdt, G., Bentley, M. J., Pritchard, H. D., Brown, J., Conway, H., Drews, R., Durand, G., Goldberg, D., Hattermann, T., Kingslake, J., Lenaerts, J. T. M., Martín, C., Mulvaney, R., Nicholls, K. W., Pattyn, F., Ross, N., Scambos, T., and Whitehouse, P. L.: Antarctic ice rises and rumples: Their properties and significance for ice-sheet dynamics and evolution, Earth-Science Reviews, 150, 724–745, https://doi.org/10.1016/j.earscirev.2015.09.004, 2015.

Mayewski, P. A., Maasch, K. A., White, J. W. C., Steig, E. J., Meyerson, E., Goodwin, I., Morgan, V. I., Van Ommen, T., Curran, M. A. J., Souney, J., and Kreutz, K.: A 700 year record of Southern Hemisphere extratropical climate variability, Ann. Glaciol., 39, 127–132, https://doi.org/10.3189/172756404781814249, 2004.

Medley, B. and Thomas, E. R.: Increased snowfall over the Antarctic Ice Sheet mitigated twentieth-century sea-level rise, Nature Clim Change, 9, 34–39, https://doi.org/10.1038/s41558-018-0356-x, 2019.

Mercer, J. H.: West Antarctic ice sheet and CO2 greenhouse effect - A threat of disaster, Nature, 271, 321–325, 1978.

Morlighem, M., Rignot, E., Binder, T., Blankenship, D., Drews, R., Eagles, G., Eisen, O., Ferraccioli, F., Forsberg, R., Fretwell, P., Goel, V., Greenbaum, J. S., Gudmundsson, H., Guo, J., Helm, V., Hofstede, C., Howat, I., Humbert, A., Jokat, W., Karlsson, N. B., Lee, W. S., Matsuoka, K., Millan, R., Mouginot, J., Paden, J., Pattyn, F., Roberts, J., Rosier, S., Ruppel, A., Seroussi, H., Smith, E. C., Steinhage, D., Sun, B., den Broeke, M. R. van, Ommen, T. D. van, van Wessem, M., and Young, D. A.: Deep glacial troughs and stabilizing ridges unveiled beneath the margins of the Antarctic ice sheet, Nature Geoscience, 13, 132–137, https://doi.org/10.1038/s41561-019-0510-8, 2020.

Neff, P.: Amundsen Sea Coastal Ice Rises: Future Sites for Marine-Focused Ice Core Records, Oceanog, 33, https://doi.org/10.5670/oceanog.2020.215, 2020.

O'Connor, G., Nakayama, Y., Steig, E., Armour, K., Thompson, L., Hyogo, S., Berdahl, M., and Shimada, T.: Enhanced West Antarctic ice loss triggered by polynya response to meridional winds, 18, 840–847, https://doi.org/10.5194/egusphere-egu25-13728, 2025.

Orsi, A. J., Cornuelle, B. D., and Severinghaus, J. P.: Little Ice Age cold interval in West Antarctica: Evidence from borehole temperature at the West Antarctic Ice Sheet (WAIS) Divide: WAIS DIVIDE TEMPERATURE, Geophys. Res. Lett., 39, n/a-n/a, https://doi.org/10.1029/2012GL051260, 2012.

https://doi.org/10.5194/egusphere-2025-6010
Preprint. Discussion started: 17 December 2025
© Author(s) 2025. CC BY 4.0 License.

Paolo, F. S., Padman, L., Fricker, H. A., Adusumilli, S., Howard, S., and Siegfried, M. R.: Response of Pacific-sector Antarctic ice shelves to the El Niño/Southern Oscillation, Nature Geosci, 11, 121–126, https://doi.org/10.1038/s41561-017-0033-0, 2018.

Petty, A. A., Feltham, D. L., and Holland, P. R.: Impact of Atmospheric Forcing on Antarctic Continental Shelf Water Masses, Journal of Physical Oceanography, 43, 920–940, https://doi.org/10.1175/JPO-D-12-0172.1, 2013.

Rowell, I., Martin, C., Mulvaney, R., Pryer, H., Tetzner, D., Doyle, E., Talasila, H. M., Li, J., and Wolff, E.: An age scale for new climate records from Sherman Island, West Antarctica, Clim. Past, 19, 1699–1714, https://doi.org/10.5194/cp-19-1699-2023, 2023.

Schwanck, F., C. Simões, J., Handley, M., A. Mayewski, P., D. Auger, J., T. Bernardo, R., and E. Aquino, F.: A 125-year record of climate and chemistry variability at the Pine Island Glacier ice divide, Antarctica, Ice Cores, https://doi.org/10.5194/tc-2016-242, 2016.

Smith, B., Fricker, H. A., Gardner, A. S., Medley, B., Nilsson, J., Paolo, F. S., Holschuh, N., Adusumilli, S., Brunt, K., Csatho, B., Harbeck, K., Markus, T., Neumann, T., Siegfried, M. R., and Zwally, H. J.: Pervasive ice sheet mass loss reflects competing ocean and atmosphere processes, Science, 368, 1239–1242, https://doi.org/10.1126/science.aaz5845, 2020.

Steig, E. J. and Neff, P. D.: The prescience of paleoclimatology and the future of the Antarctic ice sheet, Nat Commun, 9, https://doi.org/10.1038/s41467-018-05001-1, 2018.

Steig, E. J., Schneider, D. P., Rutherford, S. D., Mann, M. E., Comiso, J. C., and Shindell, D. T.: Warming of the Antarctic ice-sheet surface since the 1957 International Geophysical Year, Nature, 457, 459–462, https://doi.org/10.1038/nature07669, 2009.

Steig, E. J., Ding, Q., Battisti, D. S., and Jenkins, A.: Tropical forcing of Circumpolar Deep Water Inflow and outlet glacier thinning in the Amundsen Sea Embayment, West Antarctica, Ann. Glaciol., 53, 19–28, https://doi.org/10.3189/2012AoG60A110, 2012.

Steig, E. J., Ding, Q., White, J. W. C., Küttel, M., Rupper, S. B., Neumann, T. A., Neff, P. D., Gallant, A. J. E., Mayewski, P. A., Taylor, K. C., Hoffmann, G., Dixon, D. A., Schoenemann, S. W., Markle, B. R., Fudge, T. J., Schneider, D. P., Schauer, A. J., Teel, R. P., Vaughn, B. H., Burgener, L., Williams, J., and Korotkikh, E.: Recent climate and ice-sheet changes in West Antarctica compared with the past 2,000 years, Nature Geosci, 6, 372–375, https://doi.org/10.1038/ngeo1778, 2013.

Thomas, E. R., Bracegirdle, T. J., Turner, J., and Wolff, E. W.: A 308 year record of climate variability in West Antarctica, Geophysical Research Letters, 40, 5492–5496, https://doi.org/10.1002/2013gl057782, 2013.

Thomas, E. R., Van Wessem, J. M., Roberts, J., Isaksson, E., Schlosser, E., Fudge, T. J., Vallelonga, P., Medley, B., Lenaerts, J., Bertler, N., Van Den Broeke, M. R., Dixon, D. A., Frezzotti, M., Stenni, B., Curran, M., and Ekaykin, A. A.: Regional Antarctic snow accumulation over the past 1000 years, Clim. Past, 13, 1491–1513, https://doi.org/10.5194/cp-13-1491-2017, 2017.

Thompson, D. W. J. and Wallace, J. M.: Regional Climate Impacts of the Northern Hemisphere Annular Mode, Science, 293, 85–89, https://doi.org/10.1126/science.1058958, 2001.

https://doi.org/10.5194/egusphere-2025-6010
Preprint. Discussion started: 17 December 2025
© Author(s) 2025. CC BY 4.0 License.

Trenberth, K. and National Center for Atmospheric Research Staff (eds): The Climate Data Guide: Nino SST Indices (Nino 1+2, 3, 3.4, 4; ONI and TNI)., 2025.

Trenberth, K. E.: The Definition of El Niño, Bull. Amer. Meteor. Soc., 78, 2771–2777, https://doi.org/10.1175/1520-0477(1997)078%253C2771:tdoeno%253E2.0.co;2, 1997.

Tsukernik, M. and Lynch, A. H.: Atmospheric Meridional Moisture Flux over the Southern Ocean: A Story of the Amundsen Sea, Journal of Climate, 26, 8055–8064, https://doi.org/10.1175/JCLI-D-12-00381.1, 2013.

Turner, J.: The El Niño–southern oscillation and Antarctica, Intl Journal of Climatology, 24, 1–31, https://doi.org/10.1002/joc.965, 2004.

Turner, J., Phillips, T., Hosking, J. S., Marshall, G. J., and Orr, A.: The Amundsen Sea low, Intl Journal of Climatology, 33, 1818–1829, https://doi.org/10.1002/joc.3558, 2013.

Turner, J., Orr, A., Gudmundsson, G. H., Jenkins, A., Bingham, R. G., Hillenbrand, C. D., and Bracegirdle, T. J.: Atmosphere–ocean–ice interactions in the Amundsen Sea Embayment, West Antarctica, Reviews of Geophysics, 55, 235–276, https://doi.org/10.1002/2016RG000532, 2017.

Wille, J. D., Favier, V., Dufour, A., Gorodetskaya, I. V., Turner, J., Agosta, C., and Codron, F.: West Antarctic surface melt triggered by atmospheric rivers, Nat. Geosci., 12, 911–916, https://doi.org/10.1038/s41561-019-0460-1, 2019.

Winski, D. A., Fudge, T. J., Ferris, D. G., Osterberg, E. C., Fegyveresi, J. M., Cole-Dai, J., Thundercloud, Z., Cox, T. S., Kreutz, K. J., Ortman, N., Buizert, C., Epifanio, J., Brook, E. J., Beaudette, R., Severinghaus, J., Sowers, T., Steig, E. J., Kahle, E. C., Jones, T. R., Morris, V., Aydin, M., Nicewonger, M. R., Casey, K. A., Alley, R. B., Waddington, E. D., Iverson, N. A., Dunbar, N. W., Bay, R. C., Souney, J. M., Sigl, M., and McConnell, J. R.: The SP19 chronology for the South Pole Ice Core – Part 1: volcanic matching and annual layer counting, Clim. Past, 15, 1793–1808, https://doi.org/10.5194/cp-15-1793-2019, 2019.

Winstrup, M., Vallelonga, P., Kjær, H. A., Fudge, T. J., Lee, J. E., Riis, M. H., Edwards, R., Bertler, N. A. N., Blunier, T., Brook, E. J., Buizert, C., Ciobanu, G., Conway, H., Dahl-Jensen, D., Ellis, A., Emanuelsson, B. D., Hindmarsh, R. C. A., Keller, E. D., Kurbatov, A. V., Mayewski, P. A., Neff, P. D., Pyne, R. L., Simonsen, M. F., Svensson, A., Tuohy, A., Waddington, E. D., and Wheatley, S.: A 2700-year annual timescale and accumulation history for an ice core from Roosevelt Island, West Antarctica, Clim. Past, 15, 751–779, https://doi.org/10.5194/cp-15-751-2019, 2019.

Zhu, J., Xie, A., Qin, X., Wang, Y., Xu, B., and Wang, Y.: An Assessment of ERA5 Reanalysis for Antarctic Near-Surface Air Temperature, Atmosphere, 12, 217, https://doi.org/10.3390/atmos12020217, 2021.